الجمهورية الجزائرية الديمقراطية الشعبية
وزارة التعليم العالي والبحث العلمي

People's Democratic Republic of Algeria
Ministry of Higher Education and Scientific Research
Saad Dahleb University – Blida 1

Faculty of Natural and Life Sciences

Department of Biology

Final Year Thesis submitted in partial fulfillment of the requirements for the Master's Degree

Specialty: Pharmacotoxicology

Presented by:

NEMDIL Samira

Title:

Pharmacological Study of a Nanoencapsulated System and Histopathological Analysis

Defended before the jury:

Dr. RAHIM I.	University of Blida 1	**Chairperson**
Dr. BOULESNAM L. S.	University of Blida 1	**Examiner**
Dr. AYACHI N.	University of Blida 1	**Supervisor**
PhD Candidate BOULAIOUNE A.	University of Blida 1	**Co-supervisor**

Academic year: **2024-2025**

Abstract

This study is part of the promotion of innovative approaches in wound healing and nanomedicine. It focuses on the synthesis, formulation, and evaluation of a transdermal silver nanoparticles-based patches, designed to accelerate tissue regeneration while minimizing infection risk.

Silver nanoparticles (AgNPs) were synthesized using a solvent-free mechanochemical technique and incorporated into a polymer-based biofilm patch. The synthesized nanoparticles were characterized by UV-vis spectroscopy, dynamic light scattering (DLS), and zeta potential analysis, confirming particle formation with adequate stability and size distribution.

An ex vivo permeability study using Franz diffusion cell demonstrated sustained AgNPs release through excised mouse skin, validating its ability to penetrate the cutaneous barrier. In in vivo tests, full-thickness wounds were induced in Wistar rats and treated with the AgNPs-based patches. Compared to control and commercial reference treatment (Cicatryl®), the AgNPs-treated group exhibited accelerated healing with over 89% wound contraction by day 5, and complete closure by day 21.

Histological analyses confirmed early re-epithelialization, organized collagen matrix, and reappearance of skin appendages in the AgNPs-treated group, suggesting enhanced regenerative activity. These findings confirm the regenerative potential of AgNPs-based systems and highlight their relevance in modern pharmacological wound management.

Keywords: Silver nanoparticles, transdermal patch, wound healing, histology, Franz diffusion cell.

Résumé

Cette étude s'inscrit dans la promotion des approches innovantes en cicatrisation et en nanomédecine. Elle porte sur la synthèse, la formulation et l'évaluation de patchs transdermiques à base de nanoparticules d'argent, conçus pour accélérer la régénération tissulaire tout en minimisant le risque d'infection.

Les nanoparticules d'argent (AgNPs) ont été synthétisées par une technique mécanochimique sans solvant, puis incorporées dans un patch à base de polymère. Les nanoparticules synthétisées ont été caractérisées par spectroscopie UV-visible, diffusion dynamique de la lumière (DLS) et analyse du potentiel zêta, confirmant la formation de particules avec une stabilité et une distribution de taille adéquates.

Une étude de perméabilité ex vivo à l'aide d'une cellule de Franz a démontré une libération prolongée des AgNPs à travers une peau de souris excisée, validant leur capacité à traverser la barrière cutanée. Lors des tests in vivo, des plaies à pleine épaisseur ont été induites chez des rats Wistar, puis traitées avec les patchs transdermiques à base d'AgNPs. Comparé au groupe témoin et au traitement de référence commercial (Cicatryl®), le groupe traité par les patchs de AgNPs a montré une cicatrisation accélérée avec plus de 89% de contraction de la plaie dès le jour 5, et une fermeture complète au jour 21.

Les analyses histologiques ont confirmé une réépithélisation précoce, une matrice de collagène bien organisée, ainsi que la réapparition des compartiments cutanées chez le groupe traité avec les patchs de AgNPs, suggérant une activité régénérative renforcée. Ces résultats confirment le potentiel régénératif des systèmes à base d'AgNPs, et soulignent leur intérêt dans la prise en charge pharmacologique moderne des plaies.

Mots-clés : Nanoparticules d'argent, patch transdermique, cicatrisation, histologie, cellule de Franz.

الملخص

هذه الدراسة تندرج ضمن إطار تعزيز الأساليب المبتكرة في التئام الجروح والنانومعالجة .وتركّز على تخليق، تركيب وتقييم لصقات عبر الجلد تعتمد على جسيمات الفضة النانوية، صُممت لتسريع تجديد الأنسجة مع تقليل خطر العدوى.

تم تصنيع جسيمات الفضة النانوية باستخدام تقنية ميكانيائية كيميائية خالية من المذيبات، وتم دمجها في لصقة بيوفيلمية قائمة على البوليمرات .وقد تم توصيف الجسيمات المصنعة باستخدام التحليل الطيفي بالأشعة فوق البنفسجية والمرئية، وتشتت الضوء الديناميكي، وتحليل الجهد السطحي ، مما أكد تكوين الجسيمات بثبات وتوزيع .حجمي مناسبين

أظهرت دراسة النفاذية خارج الجسم باستخدام خلية فرانز للانتشار إطلاقًا مستمرًا للجسيمات عبر جلد فأر منزوع، مما أثبت قدرتها على اختراق الحاجز الجلدي .وفي الاختبارات الحيوية، تم إحداث جروح عميقة في فئران ويستار، وعولجت باستخدام لصقات .وبالمقارنة مع المجموعة الضابطة والعلاج المرجعي التجاري، أظهر الفريق المعالج تسارعًا ملحوظًا في التئام الجروح، حيث تجاوزت نسبة الانكماش 89٪ بحلول اليوم الخامس، مع إغلاق تام في .اليوم الحادي والعشرين

أكدت التحاليل النسيجية حدوث إعادة التظهير في وقت مبكر، وتنظيم مصفوفة الكولاجين، وعودة الزوائد الجلدية في مجموعة ، مما يشير إلى نشاط تجديدي معزز .هذه النتائج تؤكد الإمكانات المحفّزة للتجديد لأنظمة، .وتبرز أهميتها في الإدارة الصيدلانية الحديثة للجروح

الكلمات المفتاحية :جسيمات الفضة النانوية، لصقة عبر الجلد، التئام الجروح، التحليل النسيجي، خلية فرانز .للانتشار

Acknowledgement

I thank Allah, the Almighty, for granting us the courage, willpower, and patience to complete this work.

I express our deepest gratitude to my supervisor, ***Dr. Nabila Ayachi****, for her constant availability, kind guidance, insightful advice, and the valuable time she devoted to us throughout the development of this thesis.*

I also warmly thank my co-supervisor, ***PhD Candidate Abderrahmane Boulaioune****, for his continuous support, encouragement, and scientific contributions that have greatly enriched this research.*

my sincere appreciation goes to the chairperson of the jury, ***Dr. Rahim I.,*** *for the honor of presiding over the evaluation of this work. Her presence and valuable comments were of great importance to the improvement of this study.*

I also extend our respectful thanks to ***Dr. Boulesnam L. S.,*** *jury examiner, for her careful reading of this thesis and her constructive and insightful remarks.*

I express my sincere gratitude to ***Professor Hadj Sadok A.,*** *Director of the LAFPC Laboratory, for his guidance*

I would like to thank ***PhD Candidate Amtsif Anis*** *for his valuable assistance and insightful advice throughout the development of this thesis.*

I'm especially grateful to ***Ms. Drias Nour*** *during the more demanding stages of this work.*

I wish to sincerely thank my family for their unwavering support. Their unconditional love, patience, and faith have been my foundation

Dedication

Alhamdulillah, always and forever, for His countless blessings
for what I have become, for the strength He has given me,
and for every step that led me to this moment.

*To my gentle mother **Nabila**, my refuge and my light*
thank you for your unconditional love and silent prayers.

*To my father **Sidahmed**, for your unwavering support, thank you from the bottom of my heart.*

*To my twin sister, **Amira**, whose bond and presence have been a constant source of strength.*

*To my older sisters, **Bahia** and **Imene**, thank you for your unwavering support, wise guidance, and sincere belief in me.*

*To my cherished friends **Hadil, Randa, Meriem, Khaoula, Chaima, Maria,***
***Asma, Lydia,** and **Katia,** your kindness, encouragement, and joyful moments have lightened this journey in more ways than one.*

*And to everyone who has crossed my path and believed in me, **THANK YOU***

Table of contents

Table of figures

Table of tables

General Introduction

General Introduction

The skin, as the largest organ of the human body, serves as a critical barrier against external aggressions, regulates temperature, and participates in immunological surveillance (**Proksch E., et al., 2008**). Its complex structure, comprising the epidermis, dermis, and hypodermis, is intricately designed to support these functions. Among the most significant challenges facing skin integrity is the process of wound healing, a dynamic and highly regulated sequence of events involving hemostasis, inflammation, proliferation, and remodeling. This orchestrated cascade ensures tissue repair and the restoration of barrier function, but it can be delayed or impaired under pathological conditions such as infection or chronic inflammation **(Guo S., et al., 2010).**

Recent advances in nanotechnology have opened new frontiers in the development of innovative wound care strategies. Nanoparticles, owing to their unique physicochemical properties, have demonstrated significant potential in enhancing the efficacy of wound healing agents. (**Rai M., et al., 2009**). Among these, silver nanoparticles (AgNPs) have attracted considerable attention due to their broad-spectrum antimicrobial activity, anti-inflammatory effects, and ability to promote tissue regeneration (**Franci G., et al., 2015**). AgNPs can be synthesized via chemical, physical, and green synthesis using plant extracts (**Ibrahim H. M., 2015**). Chemical reduction is the most common used technique due to its simplicity and efficiency, using agents to reduce Ag^{+} ions to Ag^{0}, and stabilizers such as polymers to prevent aggregation (**Ahmed S., et al., 2016**).

To confirm the formation of AgNPs, proper characterization is crucial to determine nanoparticle size, shape, and stability, such as UV-vis spectroscopy, dynamic light scattering, and zeta potential help confirm key properties influencing their biological activity (**Song J., et al., 2009; Duman H., et al., 2024**).

To improve delivery, AgNPs can be incorporated into transdermal patches, which enable sustained release through the skin. These systems, often based on biopolymers like chitosan or alginate, improve bioavailability, reduce systemic exposure at the wound site (**Prausnitz M. R., and Langer R., 2008; Monteiro D. R., et al., 2022**), and ability to accelerate healing and reduce the risk of infection, marking a significant evolution in wound care technology (**Lansdown A. B. G., 2006**).

The main objective of this research is to perform a pharmacological investigation of a nanoencapsulated system and support the findings with histopathological analysis. The formulation was assessed using an in vivo model involving Wistar rats, and the therapeutic effects were further supported by histopathological evaluation of skin tissue following a 21-day treatment protocol. In addition to evaluating healing efficacy, permeability assays were performed using mouse skin to investigate the ability of AgNPs to diffuse through the stratum corneum and reach deeper dermal layers. These ex vivo assays provided critical insights into the penetration profile and potential bioavailability of silver nanoparticles, validating their transdermal delivery and therapeutic relevance. Ultimately, this study seeks to underscore the biomedical relevance and innovative potential of AgNPs-based systems as emerging tools in regenerative medicine and dermal pharmacotherapy.

This thesis is organized into three chapters:

The **first chapter** is a literature review, divided into three sections. The first provides a general overview of skin anatomy and physiology, focusing on the mechanisms involved in wound repair. The second section explores the principles of nanotechnology, the synthesis and characterization of silver nanoparticles, and their biomedical applications. The third section explains particularly the incorporation of AgNPs into transdermal patches.

The **second chapter** details the description of the experimental methodology, encompassing the materials, animal protocol, and analytical techniques employed throughout the study.

Finally, the **third chapter** presents the results obtained, followed by their interpretation and scientific discussion.

The manuscript concludes with a general conclusion and perspectives for future research.

Chapter I:
Literature review

Chapter I: Literature review

I.1. An Overview of Skin

I.1.1. Skin

As the largest organ of the body, composed of water, protein, fats, and minerals, the skin plays a crucial role (Cleveland Clinic., 2023) in keeping vital chemicals and nutrients in the body while providing a barrier against dangerous substances (Benedetti J., 2024) safeguarding the body from pathogens, and maintaining thermal balance. Additionally, the nerves embedded in the skin allow us to perceive sensations such as heat and cold (Cleveland Clinic, 2023).

I.1.2. Anatomy

The skin of the human body covers a surface area of approximately 1.6 m^2 and accounts for about 16% of an adult's body weight (Shimizu H., 2017).

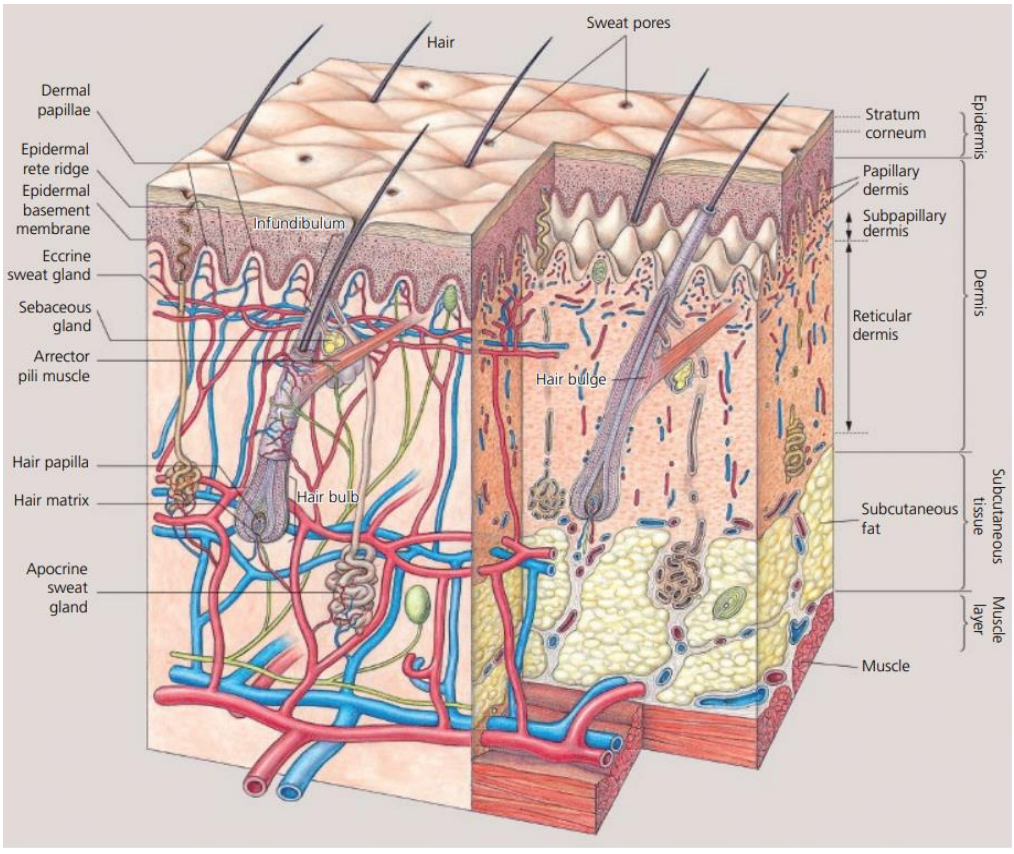

Figure 1: Structure of the skin (Shimizu H., 2017)

I.1.3. Skin composition and function

The skin is a vital protective barrier between the internal environment and external factors. It comprises three primary layers: the epidermis, dermis, and hypodermis. These layers provide mechanical protection, immune defense, and several other essential functions.

I.1.3.1. Epidermis

The epidermis is the outermost layer of the skin. with an average thickness of approximately 0.2 mm (Shimizu H., 2017). The principal cell is the keratinocyte (95% of cells). Melanocytes, Langerhans cells, and Merkel cells account for the remaining 5% (Lai-Cheong J., et al., 2013).

The epidermis is divided into five main layers depending on the state of keratinocyte differentiation (Lai-Cheong J., et al., 2013). The epidermis is avascular, meaning it lacks blood vessels, and relies on the dermis for nutrient supply (Mohamed H., et al., 2022; Gilaberte Y., et al., 2016).

- **Layers of the Epidermis**

The keratinocytes are arranged in five main layers:

1- Stratum basale (basal layer)

The basal layer is composed of a single row of columnar or cuboidal cells. These cells are mitotically active, giving rise to keratinocytes that migrate upward. Melanocytes reside here, producing melanin transferred to adjacent keratinocytes, while Merkel cells contribute to mechanoreception (Ita K., 2020; Gilaberte Y., et al., 2016; Shimizu H., 2017; Wysocki A., et al., 2006; Lotfollahi Z., 2024).

2- Stratum spinosum (prickle cell layer)

Comprising 5 to 10 layers of keratinocytes that are connected by desmosomes (Shimizu H., 2017). This layer provides mechanical strength and hosts Langerhans cells for immune surveillance (Gilaberte Y., et al., 2016; Venus M., et al., 2010).

3- Stratum granulosum (granular layer)

Consists of 2–3 layers of flattened keratinocytes containing intracellular granules of keratohyalin. The cytoplasm also contains smaller lamellated granules (Odland bodies). The cells discharge their lipid components into the intercellular space (Shimizu H., 2017), which plays an important role in barrier function which preventing water loss (Ita K., 2020; Gilaberte Y., et al., 2016).

4- Stratum corneum (horny layer)

The outermost layer comprises 15–30 layers of enucleated, flattened corneocytes. These cells are embedded in a lipid matrix, forming a durable and hydrophobic barrier that protects underlying tissues and prevents trans-epidermal water loss (Gilaberte Y., et al. ,2016; Ita K., 2020; Lotfollahi, Z., 2024; Wysocki A., et al., 2006).

5- Stratum Lucidum

A thin, clear layer found in the palms, soles, and fingertips. It consists of transparent keratinocytes and acts as an additional barrier present only in thick skin (Lotfollahi Z., 2024; Wysocki A., et al., 2006).

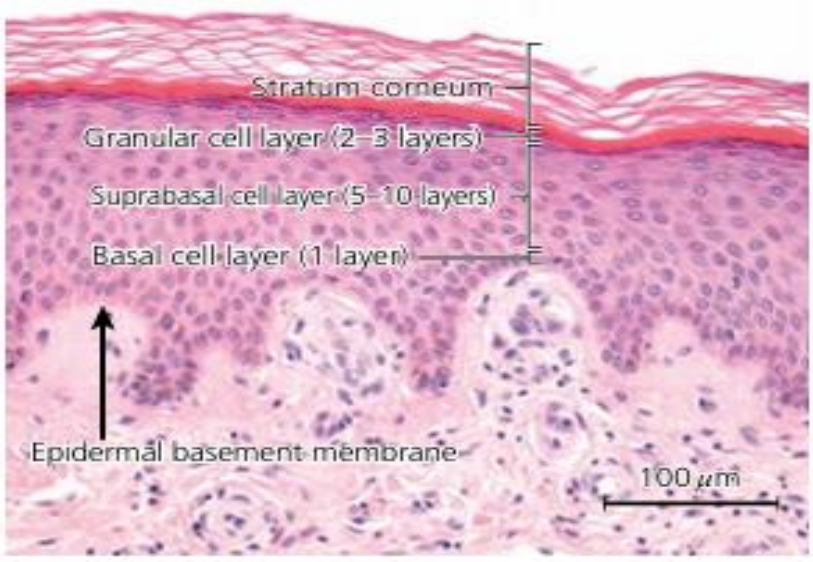

Figure 2: The four layers of the epidermis (Shimizu H., 2017)

I.1.3.2. Dermis

The dermis is the thick, fibrous middle layer of the skin, located between the epidermis and hypodermis. It serves as the skin's main supportive and nutritive layer, playing a vital role in mechanical strength, thermoregulation, sensation, immune surveillance, and wound healing (Kolarsick P. A. J., et al., 2006; Shimizu H., 2017).

The dermis is primarily composed of collagen (70–80% dry weight), elastin fibers, and extracellular matrix (ECM), which contains glycosaminoglycans (GAGs) and proteoglycans. These elements contribute to the dermis's strength, elasticity, and hydration (Venus M., et al., 2010; Wysocki A., et al., 2006). Fibroblasts are the most prevalent cell type, responsible for producing and maintaining ECM components, including type I and III collagen (Gilaberte Y., et al., 2016; Shimizu H., 2017). The dermis is subdivided into three distinct layers:

1. **Papillary layer:** The papillary dermis is the superficial layer that interdigitates with the epidermis through structures called dermal papillae and rete ridges, increasing the surface area for nutrient diffusion and epidermal support (Lotfollahi Z., 2024). This layer is composed of loose connective tissue, capillary loops, lymphatic vessels, and sensory receptors, such as Meissner's corpuscles, which mediate light touch (Shimizu H., 2017; Wysocki A., et al., 2006).
2. **Subpapillary layer:** This area is subjacent to the epidermis and has the same components as the papillary layer (Shimizu H., 2017).
3. **Reticular layer:** Beneath the papillary dermis lies the reticular dermis, a dense irregular connective tissue layer rich in collagen bundles arranged in a mesh-like structure. It houses appendages such as hair follicles, sebaceous glands, eccrine and apocrine sweat glands, nerves, blood vessels, and Pacinian corpuscles, which detect deep pressure and vibration (Gilaberte Y., et al., 2016; Venus M., et al., 2010). This layer provides the skin with mechanical strength and elasticity, critical for resisting tearing and deformation (Shimizu H., 2017).

- **Glands**

The dermis contains two major types of exocrine glands:

- **Sebaceous glands:** These are holocrine glands associated with hair follicles. They secrete sebum, an oily substance that lubricates the skin and hair and has mild antimicrobial properties (Kolarsick P. A. J., et al., 2006**;** Venus M., et al., 2010).
- **Sweat glands:** There are two types of this glands:

1- **Eccrine glands:** Found throughout the body, especially on the palms, soles, and forehead. They are involved in thermoregulation by producing a watery secretion to cool the body via evaporation.

2- **Apocrine glands**: Located mainly in the axillae, groin, and areolae, these glands become active after puberty and produce a thicker, milky secretion associated with pheromonal and emotional responses (Gilaberte Y., et al., 2016).

These glands are embedded in the reticular dermis and are surrounded by a vascular and neural network for functional regulation (Wysocki A., et al., 2006**).**

➢ **Blood Vessels**

The dermis contains two horizontal vascular plexuses:

1. **The superficial plexus** (in the papillary dermis) supplies capillary loops that nourish the avascular epidermis and assist in wound healing (Lotfollahi Z., 2024).
2. **The deep plexus** (at the dermal-hypodermal junction) supplies larger vessels, eccrine glands, hair follicles, and sebaceous glands (Shimizu H., 2017).

These vessels play a critical role in thermoregulation, nutrient delivery, immune cell trafficking, and angiogenesis. The capillary loops, along with venous and lymphatic vessels, ensure efficient fluid and cellular exchange across skin compartments (Wysocki A., et al., 2006).

➢ **Functional Significance**

- **Support and structure:** The dermis gives the skin its mechanical resilience and elasticity (Venus M., et al., 2010).
- **Nutrition:** Dermal capillaries supply nutrients and oxygen to the avascular epidermis (Shimizu H., 2017).
- **Thermoregulation:** Blood vessels dilate or constrict to control heat loss (Wysocki A., et al., 2006).
- **Sensation:** Sensory receptors detect environmental stimuli (Gilaberte Y., et al., 2016).

- **Wound healing**: Dermal fibroblasts and immune cells are key players in tissue regeneration and inflammation resolution (Lotfollahi Z., 2024).

I.1.3.3. Hypodermis (Subcutaneous Tissue)

The hypodermis, also referred to as the subcutaneous tissue or panniculus, is the deepest layer of the skin. It lies beneath the dermis and serves as a crucial interface between the skin and underlying muscles, bones, and organs (Kolarsick P. A. J., et al., 2006).

The hypodermis is composed predominantly of adipose tissue arranged in lobules separated by fibrous connective tissue septa. These septa contain collagen fibers, elastic fibers, blood vessels, lymphatics, and nerve bundles (Shimizu H., 2017). The adipocytes in this layer store triglycerides, which provide a reserve of metabolic energy for the body (Gilaberte Y., et al., 2016).

The thickness of the hypodermis varies by anatomical location, age, sex, and nutritional status. It is thickest in regions such as the buttocks, thighs, and abdomen, and thinnest in areas like the eyelids (Wysocki A., et al., 2006).

➢ **Adipose Tissue (Fat Cells)**

The predominant cell type in the hypodermis is the adipocyte, which stores energy in the form of triglycerides. These fat cells are arranged in lobules, which are separated by fibrous connective tissue septa (Gilaberte Y., et al., 2016). The adipose layer functions as:

a. **An energy reservoir**, releasing fatty acids during metabolic demand;
b. **A thermal insulator**, helping maintain core body temperature;
c. **A shock absorber**, cushioning underlying muscles, bones, and organs from mechanical injury (Lotfollahi Z., 2024).

Adipose tissue also acts as an endocrine organ, secreting hormones such as leptin, adiponectin, and resistin, which regulate metabolism, inflammation, and insulin sensitivity (Wysocki A., et al., 2006).

➢ **Connective Tissue**

The adipocytes are surrounded and supported by a loose connective tissue network that includes:

- **Collagen fibers:** (mainly Type I and III), which offer tensile strength;
- **Elastin fibers:** provide elasticity and flexibility to the skin and underlying tissues;
- **Fibroblasts**: which produce and remodel the extracellular matrix;

- **Blood vessels and lymphatics:** which supply oxygen and nutrients while facilitating immune surveillance and fluid balance (Shimizu H., 2017).

This connective tissue network serves as a scaffold, anchoring the skin to underlying structures such as muscle and fascia, while also allowing mobility and resistance to shear forces (Venus M., et al., 2010).

➢ **Functions of the Hypodermis**

- **Thermal Insulation:** Adipose tissue reduces heat loss by insulating the body, thus aiding in thermoregulation, particularly in colder environments (Lotfollahi Z., 2024).
- **Mechanical Cushioning:** It provides shock absorption, protecting underlying muscles, bones, and internal organs from mechanical trauma (Gilaberte Y., et al., 2016).
- **Energy Storage:** Triglycerides stored in adipocytes are metabolically active and serve as a long-term energy reserve (Kolarsick P. A. J., et al., 2006).
- **Hormonal Activity:** Adipose tissue functions as an endocrine organ, releasing hormones such as leptin, adiponectin, and cytokines, which influence appetite, metabolism, and inflammation (Wysocki A., et al., 2006).
- **Support of Dermal Structures:** The hypodermis anchors the dermis to underlying tissues and provides pathways for larger blood vessels, lymphatic channels, and nerves that branch into the dermis and epidermis (Shimizu H., 2017).

➢ **Accessory Structures of the Skin**

Accessory structures, also known as cutaneous appendages, originate from the epidermis but extend into the dermis or hypodermis. These structures play essential roles in protection, thermoregulation, sensation, and homeostasis (Kolarsick P. A. J., et al., 2006; Shimizu H., 2017).

- **Hair Follicles**

Hair follicles are tubular invaginations of the epidermis that extend into the dermis or hypodermis. Each follicle contains a hair bulb at its base, which surrounds the dermal papilla, a vascular structure supplying nutrients to the actively dividing matrix keratinocytes (Gilaberte Y., et al., 2016). The arrector pili muscle connects to the follicle, allowing piloerection in response to cold or stress known as goosebumps (Shimizu H., 2017).

Hair functions in thermoregulation, UV protection, and tactile sensation, especially in areas with high follicle density like the scalp and face (Wysocki A., et al., 2006).

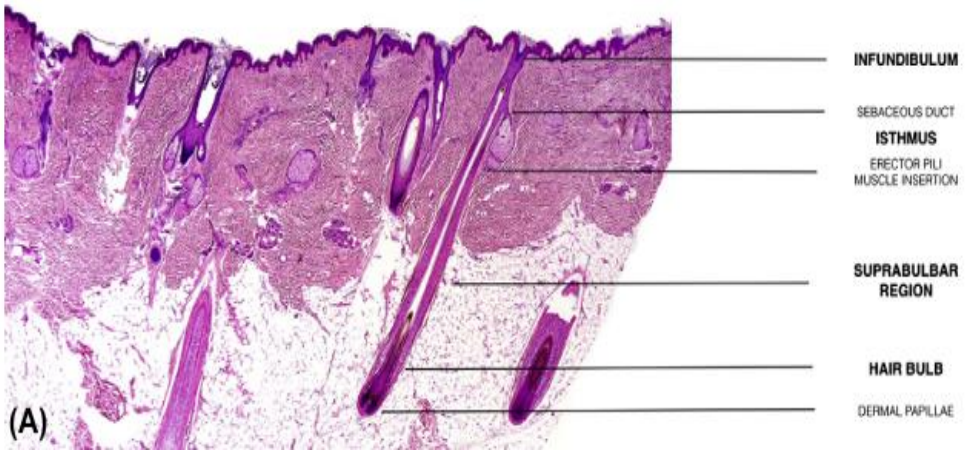

Figure 3: Terminal hair follicles in a skin biopsy of the scalp (Gilaberte Y., et al., 2016)

I.1.4. Physiology of the Skin

The skin functions as a dynamic interface between the internal and external environments. It performs a variety of physiological roles that are critical for survival, including protection, temperature regulation, sensory detection, immune defense, and metabolic activity (Kolarsick P. A. J., et al., 2006; Wysocki A., et al., 2006).

- **Protective Function**

The epidermis, particularly the stratum corneum, acts as a physical and chemical barrier. It prevents the entry of pathogens, allergens, and harmful chemicals while also reducing transepidermal water loss (TEWL) (Shimizu H., 2017). Tight junctions, desmosomes, and a lipid matrix between corneocytes maintain skin integrity (Gilaberte Y., et al., 2016).

Melanin, produced by melanocytes, protects the skin from ultraviolet (UV) radiation by absorbing harmful rays and neutralizing reactive oxygen species (Lotfollahi Z.,2024). Sebum also contributes to antimicrobial defense and maintains the skin's slightly acidic pH (4.5–5.5), which inhibits bacterial growth (Venus M., et al., 2010).

- **Thermoregulation**

Thermoregulation is controlled through sweating and cutaneous blood flow. Eccrine sweat glands, activated by sympathetic cholinergic innervation, release sweat to the skin surface where

it evaporates and cools the body (Wysocki A., et al., 2006). In cold environments, vasoconstriction of dermal blood vessels limits heat loss, while vasodilation during heat exposure increases heat dissipation (Gilaberte Y., et al., 2016). The hypodermis also insulates the body through its adipose layer (Shimizu A., 2017).

- **Sensory Perception**

The skin contains a wide array of sensory receptors that detect temperature, pressure, pain, and touch. These include:

- **Merkel cells:** detect light touch and texture;
- **Meissner's corpuscles:** sensitive to gentle pressure and vibration;
- **Pacinian corpuscles**: detect deep pressure and high-frequency vibration;
- **Free nerve endings:** respond to pain and temperature (Lotfollahi Z.,2024).

These signals are transmitted to the central nervous system, enabling reflexive responses and environmental awareness (Kolarsick P. A. J., et al., 2006).

- **Immune Functions**

The skin is an immunological organ that provides both innate and adaptive immunity. Langerhans cells in the epidermis capture antigens and present them to T lymphocytes, initiating immune responses (Wysocki A., et al., 2006).

Mast cells, dermal dendritic cells, and macrophages participate in inflammatory responses and pathogen clearance. Keratinocytes also secrete cytokines, antimicrobial peptides, and chemokines that modulate immune activity (Gilaberte Y., et al., 2016).

- **Metabolic Functions**

1. **Vitamin D Synthesis**

Upon exposure to Ultraviolet type B radiation, 7-dehydrocholesterol in the epidermis is converted to cholecalciferol (vitamin D3), which then undergoes hepatic and renal conversion to form calcitriol, the active form of vitamin D. This hormone is essential for calcium absorption, bone health, and immune regulation (Venus M., et al., 2010).

2. **Water and Electrolyte Regulation**

The skin plays a vital role in fluid and electrolyte balance. The stratum corneum, through its lipid matrix, limits water loss while eccrine sweat glands regulate sodium and chloride excretion

during thermoregulation (Lotfollahi Z., 2024). Dysfunction of this barrier, as seen in burns or eczema, can result in dehydration and electrolyte imbalance (Wysocki A., et al., 2006).

I.1.4.1 Wound Healing Process

Wound healing is a natural physiological reaction to tissue injury. However, wound healing is not a simple phenomenon but involves a complex interplay between numerous cell types, cytokines, mediators, and the vascular system (Heather A., et al., 2023).

- **Wound Healing Phases**

1. Hemostasis Phase

The hemostasis phase is the immediate response to injury and aims to stop bleeding and establish a temporary matrix for incoming cells. Within minutes of vascular injury, vasoconstriction occurs, followed by platelet aggregation and activation. Platelets adhere to the exposed collagen via Von Willebrand factor, leading to the release of α-granules containing growth factors such as platelet-derived growth factor (PDGF), transforming growth factor-beta (TGF-β), and vascular endothelial growth factor (VEGF) (Raziyeva K., et al., 2021; Wysocki A., et al., 2006).

The resulting fibrin clot not only acts as a physical barrier to pathogens but also provides a scaffold for the migration of inflammatory and reparative cells (Reinke J. M., Sorg H., 2012). This provisional matrix is enriched with fibronectin, thrombospondin, and vitronectin, which attract neutrophils and monocytes to the site of injury (Maquart F. X., Monboiss J. C., 2014).

2. Inflammatory Phase

The inflammatory phase typically begins within a few hours post-injury and lasts for up to 72 hours. It is characterized by the infiltration of neutrophils and macrophages into the wound site. Neutrophils are the first to arrive and play a vital role in microbial clearance and debris phagocytosis, while also releasing reactive oxygen species (ROS) and proteolytic enzymes (Nourian Dehkordi A., et al., 2019).

As neutrophils undergo apoptosis, monocytes differentiate into macrophages, which are crucial for transitioning the wound from inflammation to repair. Macrophages release cytokines such as interleukin-1 (IL-1), tumor necrosis factor-alpha (TNF-α), and growth factors like VEGF and PDGF, thus initiating the next phase of healing (Raziyeva K., et al., 2021). Dysregulation of

this phase can result in chronic wounds due to persistent inflammation and impaired cellular responses. (Barhoumi T., et al., 2025)

3. Proliferative Phase

The proliferative phase begins approximately 2-3 days after injury and continues for up to two weeks. This phase is marked by several key processes: fibroblast proliferation, angiogenesis, granulation tissue formation, and re-epithelialization (Reinke J. M., Sorg H., 2012)

Fibroblasts migrate into the wound bed and produce extracellular matrix components, primarily type III collagen, and glycosaminoglycans (Wysocki A., et al., 2006). Angiogenesis, the formation of new blood vessels, is driven by VEGF and fibroblast growth factor (FGF), and is essential for supplying oxygen and nutrients to the regenerating tissue (Reinke J. M., Sorg H., 2012). Granulation tissue forms as a combination of new capillaries, ECM, and fibroblasts, creating a framework for tissue repair, concurrently, keratinocytes from the wound edges and skin appendages migrate to cover the wound surface in a process called re-epithelialization (Nourian Dehkordi A., et al., 2019).

4. Remodeling Phase (Maturation)

The final phase, remodeling, can last from several weeks to years, depending on wound severity. During this phase, type III collagen is gradually replaced by type I collagen, increasing the tensile strength of the tissue (Wysocki A., et al., 2006). Myofibroblasts, which express α-smooth muscle actin, contribute to wound contraction and scar formation.

Matrix metalloproteinases (MMPs), secreted by macrophages and fibroblasts, regulate ECM degradation, allowing for tissue remodeling and scar maturation (Maquart F. X., Monboiss J. C., 2014). Most healed adult skin wounds form scars, which are fibrotic tissues lacking the full functional and mechanical characteristics of native skin (Reinke J. M., Sorg H., 2012).

➢ **Factors Affecting Healing**

- **Age:** Elderly individuals exhibit delayed inflammatory and proliferative responses, contributing to slower healing (Wysocki A., et al., 2006).
- **Nutrition:** Deficiencies in protein, vitamin C, zinc, and iron impair fibroblast function and collagen synthesis (Wysocki A., et al., 2006).
- **Infection:** Prolonged bacterial presence disrupts healing by extending the inflammatory phase and increasing protease activity (Raziyeva K., et al., 2021).

- **Chronic Disease:** Diabetes mellitus leads to impaired angiogenesis, neuropathy, and increased susceptibility to infection, all contributing to chronic wound formation (Nourian Dehkordi A., et al., 2019).
- **Medications:** that can adversely affect healing include anticonvulsants, steroids, antibiotics, angiogenesis inhibitors, and Non-Steroidal Anti-Inflammatory Drugs (NSAIDs). Drugs known to promote healing include insulin, vitamins, thyroid hormone, and iron (Heather. A et al.,2023).

II.2. Nanotechnology and silver nanoparticles

II.2.1. Fundamentals of Nanotechnology

II.2.1.1. Definition and History of Nanotechnology

Nanotechnology is the science and engineering involved in designing, synthesizing, characterizing, and applying materials and devices whose smallest functional organization is on the nanometer scale, typically between 1 and 100 nanometers. At this scale, materials often exhibit unique physical, chemical, and biological properties not seen in their bulk counterparts (Bhushan B., 2017). Nanotechnology is one of the most promising technologies of the 21st century. It is the ability to convert nanoscience theory into useful applications by observing, measuring, manipulating, assembling, controlling, and manufacturing matter at the nanometer scale **(**Bayda S., et al., 2019). The conceptual foundation of nanotechnology was laid by physicist Richard Feynman in his 1959 lecture, "There's Plenty of Room at the Bottom", where he envisioned manipulating individual atoms and molecules. The term "nanotechnology" was later coined by Norio Taniguchi in 1974 to describe the precision machining of materials at the atomic level. Significant advancements include the invention of the scanning tunneling microscope in 1981, enabling visualization of individual atoms, and the discovery of fullerenes in 1985 and carbon nanotubes in 1991, which propelled nanotechnology research forward (Kumar B., et al., 2017).

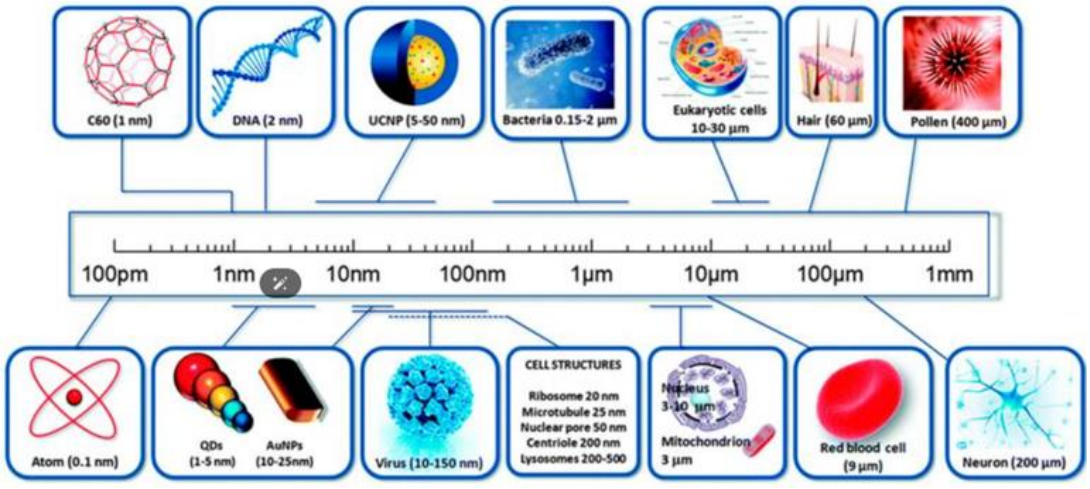

Figure 4: A comparison of the sizes of nanomaterials (Bayda S., et al., 2019)

II.2.1.2. Types of Nanomaterials

Nanomaterials are broadly classified based on their composition and structure, each with distinctive properties that qualify them for various applications.

- **Metal-Based Nanoparticles**

Metal-based nanoparticles, such as those composed of gold (Au), silver (Ag), and iron oxide (Fe_3O_4), exhibit unique optical and magnetic properties due to their nanoscale dimensions. These properties make them suitable for applications in catalysis, imaging, and drug delivery. Their high surface area-to-volume ratio enhances their reactivity and interaction with biological systems (Khan I., et al., 2019).

- **Carbon-Based Nanomaterials**

Carbon-based nanomaterials, including fullerenes, carbon nanotubes (CNTs), and graphene, are renowned for their exceptional strength, electrical conductivity, and thermal properties. These materials are being explored for use in electronics, sensors, and biomedical devices due to their unique structural and functional characteristics (Jariwala D., et al., 2014).

- **Lipid-Based and Polymeric Nanoparticles**

Lipid-based nanoparticles, such as liposomes, are widely used in drug delivery systems due to their biocompatibility and ability to encapsulate therapeutic agents. Polymeric nanoparticles, made from natural or synthetic polymers, offer controlled drug release and stability, making them valuable in pharmaceutical applications (Zielińska A., et al., 2020).

II.2.1.3. Nanoscale Properties and Behavior

At the nanoscale, materials exhibit distinct properties due to quantum effects and increased surface area-to-volume ratios. These unique properties include:

- **Optical Properties**: Nanoparticles can exhibit unique optical behaviors, such as fluorescence and surface plasmon resonance, which are utilized in imaging and sensing applications (Khan I., et al., 2019).

- **Mechanical Properties**: Nanomaterials often display enhanced strength and elasticity compared to their bulk counterparts, making them ideal for reinforcing materials **(**Taloni A., et al., 2022).
- **Chemical Reactivity**: The high surface area of nanomaterials leads to increased chemical reactivity, beneficial in catalysis and environmental applications (Bayda S., et al.,2019).
- **Magnetic Properties**: Certain nanoparticles exhibit superparamagnetism, useful in magnetic resonance imaging (MRI) and targeted drug delivery **(**Khan I., et al., 2019).

II.2.2. Synthesis of Silver Nanoparticles

II.2.2.1. Overview of Silver Nanoparticles

Silver has been employed for its antimicrobial properties since antiquity. Its historical use includes the storage of water in silver vessels and the application of silver leaf to wounds to prevent infection. During the early 20th century, particularly in World War I, silver nitrate and silver-based ointments were commonly used to treat infected wounds and burns due to their bactericidal action (Alexander J. W., 2009). These early practices laid the foundation for the modern interest in silver as an antimicrobial agent. With the advent of nanotechnology, silver has been engineered into nanoscale particles commonly known as silver nanoparticles (AgNPs). These nanoparticles exhibit enhanced surface reactivity, sustained release of silver ions, and the ability to interact with microbial membranes at the nanoscale. As such, AgNPs are now considered a superior antimicrobial alternative to traditional silver compounds (Rai M., et al., 2009).

II.2.2.2 Synthesis Methods

The synthesis of silver nanoparticles can be achieved through various methodologies, generally classified into physical, chemical, and biological (green) approaches. Each method provides unique advantages in terms of scalability, purity, cost, and environmental impact (Kumar B., et al., 2017).

- **Physical methods**

Physical methods for synthesizing silver nanoparticles include both top-down and bottom-up approaches.

Top-down techniques like laser ablation and evaporation-condensation involve breaking down bulk silver into nanoscale particles. Laser ablation, in particular, allows for high-purity nanoparticle production with precise size control but requires significant energy and specialized equipment (Sportelli M., et al., 2018).

Bottom-up physical methods, such as inert gas condensation, build nanoparticles atom by atom through the condensation of vaporized metal. These methods offer excellent control over particle size and crystallinity without chemical reagents, though they often require complex vacuum systems and are less scalable (Duman H. et al,.2024).

Another promising physical route is mechanochemical synthesis, which involves inducing chemical transformations with mechanical energy, typically through high-energy ball milling to induce solid-state reactions between precursors (McCormick P. G., et al., 2002).

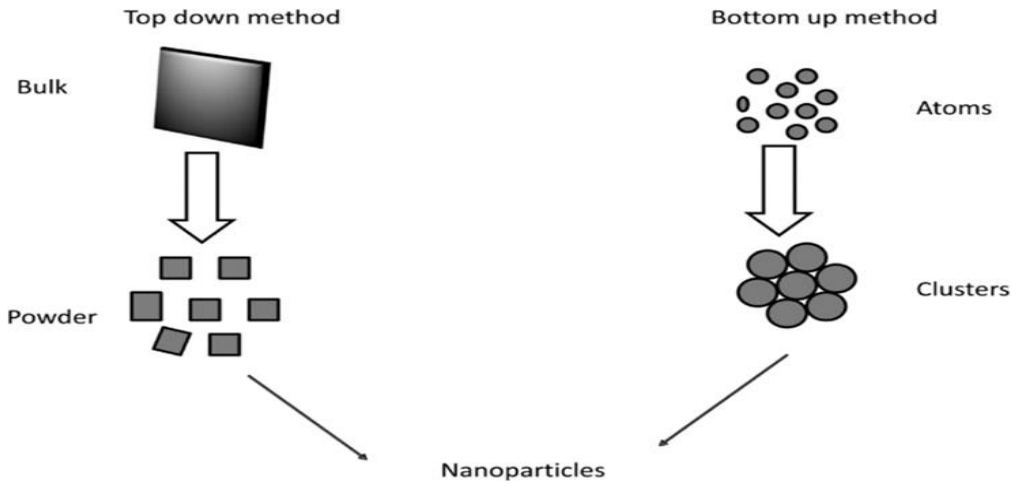

Figure 5: Top-down and bottom-up synthesis methods for nanoparticles (Duman H., et al., 2024)

- **Chemical Reduction Methods**

Chemical reduction is the most commonly used technique due to its simplicity and control. In this approach, silver ions (Ag^{+}) from a precursor such as silver nitrate ($AgNO_3$) are reduced to metallic silver (Ag^{0}) using reducing agents like sodium borohydride ($NaBH_4$), citrate, or ascorbic acid. Stabilizers such as polyvinylpyrrolidone (PVP) or chitosan are often added to prevent

nanoparticle agglomeration (Kumar B., et al., 2017). This method yields uniform, monodisperse particles, but it involves the use of hazardous chemicals that may pose environmental risks (Duman H., et al., 2024).

In recent years, mechanochemistry has emerged as a greener alternative within the field of nanoparticles synthesis, including for silver nanoparticles. Unlike traditional solution-based chemical methods, mechanochemistry induces redox reactions through mechanical force, typically by high-energy ball milling (Kováčová M., et al., 2020).

- **Green Synthesis**

Green synthesis offers an eco-friendly and sustainable alternative by using biological entities such as plant extracts, bacteria, fungi, and algae as both reducing and capping agents. These natural components contain phytochemicals like flavonoids, terpenoids, and phenolics that reduce silver ions and stabilize the nanoparticles. This method avoids the use of toxic chemicals and is biocompatible, making it ideal for biomedical applications. However, variations in biological material composition may affect the reproducibility and scale-up of AgNPs synthesis **(**Ahmed S., et al., 2016).

Among green alternatives, mechanochemistry is an emerging synthesis approach that enable the production of nanoparticles through solid-state reactions. In this solvent-free process, silver ions can be reduced in the presence of natural reducing agents such as powdered plant materials, eliminating the need for harmful solvents (Kováčová M., et al., 2020).

II.2.3. Characterization of Silver Nanoparticles

Understanding the properties of silver nanoparticles is essential for assessing their physicochemical characteristics, as detailed in Table II.1.

Table 1: Characterization Techniques for AgNPs

Characterization technique	Purpose and observations	Reference
UV-Vis Spectroscopy	Confirms AgNPs synthesis via surface plasmon resonance (SPR) peak typically at 400-450 nm.	Elbeshehy E. K. F., et al., 2015
Fourier Transform Infrared Spectroscopy (FTIR)	Identifies functional groups, hydroxyl (-OH), amine ($-NH_2$), and carbonyl (C=O) involved in AgNPs reduction and stabilization.	Ahmed S., et al., 2016
Dynamic Light Scattering (DLS)	Measures hydrodynamic diameter and polydispersity index (PDI); typical size 10–50 nm with low PDI.	Kumar B., et al., 2017
Zeta Potential Analysis	Indicates surface charge and colloidal stability; high absolute values suggest good dispersion.	Suresh A. K., et al., 2011
X-ray Diffraction (XRD)	commonly performed on dried samples in the solid state to determine their crystalline structure and purity; it shows characteristic diffraction peaks of AgNPs.	Song, J. Y., Kim, B. S., 2009
Transmission Electron Microscopy (TEM)	Visualizes morphology, size, and dispersion. Reveals spherical or other shapes between 5-20 nm.	Shankar S. S., et al., 2004

II.2.4. Biomedical Application in Dermatology

Silver nanoparticles have shown great potential in wound healing, particularly when incorporated into transdermal patches. This novel approach is gaining attention for its ability to combine antimicrobial, anti-inflammatory, and regenerative effects.

II.2.4.1. Formulation of AgNPs-Based Transdermal Patches

The preparation of silver nanoparticles-based transdermal patches involves a stepwise and controlled process to ensure uniform distribution and effective delivery of the active agent.

The process begins with the selection of suitable biocompatible polymers, typically film-forming materials such as hydroxypropyl methylcellulose (HPMC) or polyvinylpyrrolidone (PVP), which are known for their flexibility, transparency, and controlled-release properties. These polymers are dissolved in a solvent, usually ethanol or a mixture of ethanol and water, to form a homogeneous gel-like solution. Silver nanoparticles are then carefully dispersed into this polymer solution under continuous stirring or sonication to ensure even distribution throughout the matrix. Once a clear and uniform mixture is achieved, plasticizers such as glycerol or propylene glycol may be added to enhance the mechanical flexibility of the patch, while penetration enhancers like dimethyl sulfoxide (DMSO) can be included to improve skin permeation. This final formulation is then poured onto a flat surface such as a glass or Teflon-coated Petri dish and allowed to dry slowly at room temperature or under mild heating conditions, using the solvent evaporation method. During this step, an inverted funnel is often placed over the casting dish to prevent rapid solvent loss and ensure uniform film formation. After complete drying, the film is gently peeled

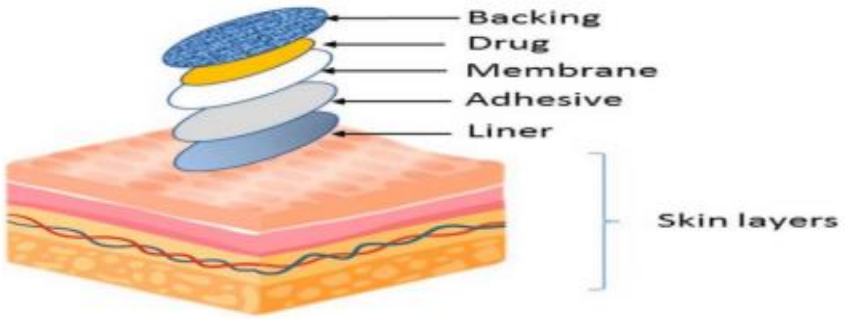

Figure 6: Layered composition of a AgNPs-based transdermal patch for wound healing (Pardhi S., et al., 2024)

off, cut into uniform rectangular patches, and stored in a desiccator to maintain stability and prevent moisture uptake. The resulting patches are thin, transparent or semi-transparent, and flexible, with embedded silver nanoparticles distributed evenly across the surface. These patches are then evaluated for key quality control parameters such as thickness, folding endurance, moisture content, drug uniformity, and tensile strength to ensure reproducibility and therapeutic reliability (Pardhi S., et al., 2024).

II.2.4.2. Mechanism of action of AgNPs-based patches in wound healing

When applied topically, silver nanoparticles-based patches act through a multifaceted mechanism that targets both infection control and tissue regeneration. AgNPs gradually release silver ions (Ag^+), which exhibit potent antimicrobial activity by disrupting bacterial membranes, binding to cellular proteins, and interfering with microbial DNA replication (Rybka M., et al., 2023). This antibacterial effect is crucial in preventing biofilm formation and managing infection, one of the primary barriers to proper wound healing (Sukweenadhi J., et al., 2023). Beyond microbial inhibition, AgNPs modulate inflammatory responses by downregulating pro-inflammatory cytokines such as TNF-α, Interleukin-1β (IL-1β), and Interleukin-6 (IL-6), effectively reducing prolonged inflammation and creating a favorable environment for tissue repair (Rybka M., et al., 2023; Nagarjuna R., et al., 2022). At the cellular level, AgNPs enhance fibroblast proliferation and keratinocyte migration, which accelerates granulation tissue formation and re-epithelialization. They also stimulate collagen deposition, contributing to stronger and more structured dermal remodeling. Importantly, AgNPs have been shown to influence the Wnt/β-catenin signaling pathway, a key regulator of skin regeneration, which promotes cell proliferation and differentiation while inhibiting apoptotic activity (Nagarjuna R., et al., 2022). These combined actions result in faster wound closure, improved structural integrity, and reduced scar formation, especially in chronic or diabetic wounds.

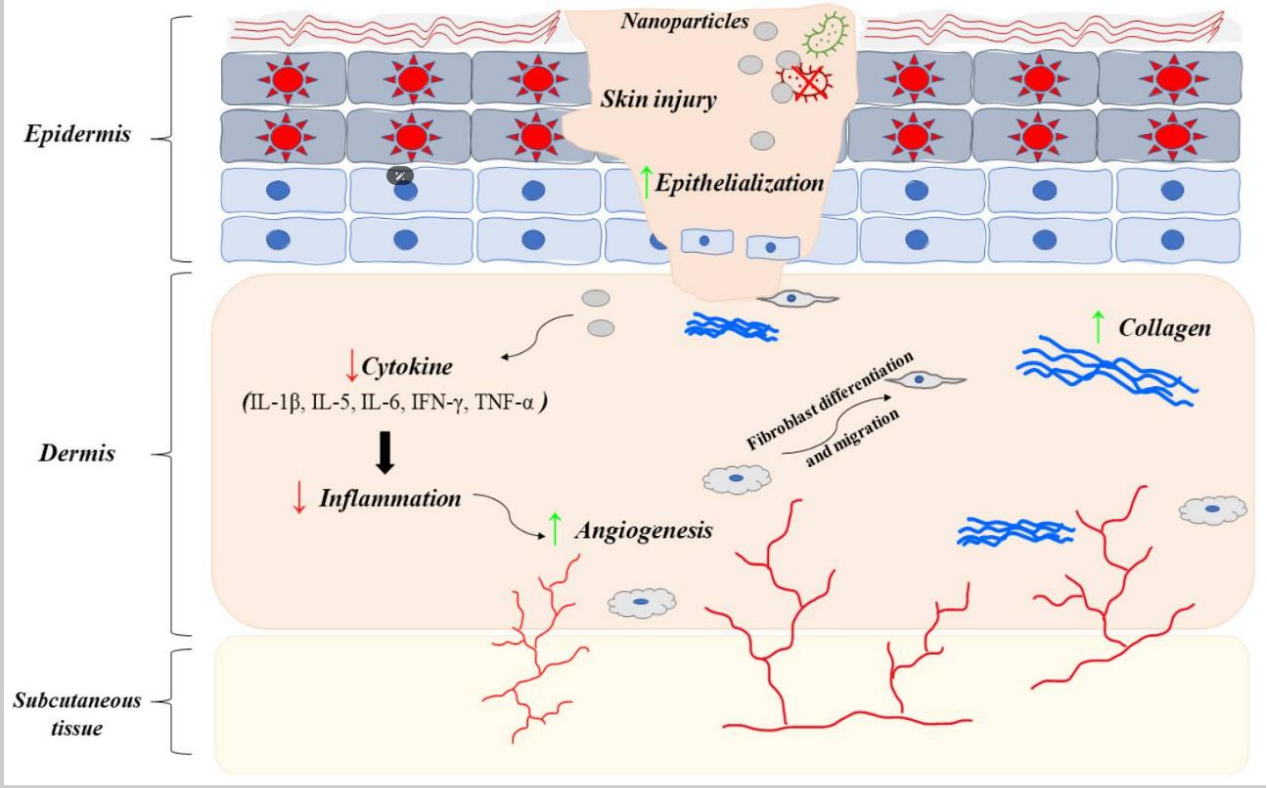

Figure 7: The healing potential of nanoparticles at the skin injury (Rybka, M., et al., 2023)

Chapter II:
Materials and Methods

Chapter II: Materials and Methods

This experimental study was conducted as part of a comprehensive pharmacological and histopathological evaluation of a transdermic silver nanoparticles-based system.

The research was conducted in multiple specialized laboratories at the University of Blida 1, along with an external facility responsible for histopathological analysis. Silver nanoparticles were synthesized and formulated in the Laboratory of Functional Analysis of Chemical Processes, where ex vivo permeability assays were also performed. The in vivo wound healing study was conducted at the experimental station of the Faculty of Natural and Life Sciences (SNV).

Histopathological evaluation of skin tissue, aimed at assessing tissue regeneration and inflammatory responses, was performed at an external laboratory (Laboratoire d'Anatomie et de Cytologie Pathologiques de Dr. Ould Slimane).

II.1. Materials

II.1.1. Biological material

The in vivo study was conducted using Wistar rats to assess the wound healing efficacy of the silver nanoparticles-based formulation using standardized ethical and experimental protocols. The characteristics of the experimental animals are presented in the table 2.

Table 2: Characteristics of rats and mice in in vivo and ex vivo assays

Species	Rat	Mice
Strain	Wistar	Albinos
Weight (g)	238–278	23
Sex	Female	Male
Number	25	12
Diet	Standard laboratory pellets	
water	Water ad libitum	

- **Housing and Acclimation Conditions**

The animals were acclimated for two weeks before the initiation of the experimental protocol, housed in Box 8 of the university's animal facility. Environmental conditions were not actively controlled; temperature and humidity fluctuated naturally within the facility and a natural 10 hours light / 14 hours dark photoperiod.

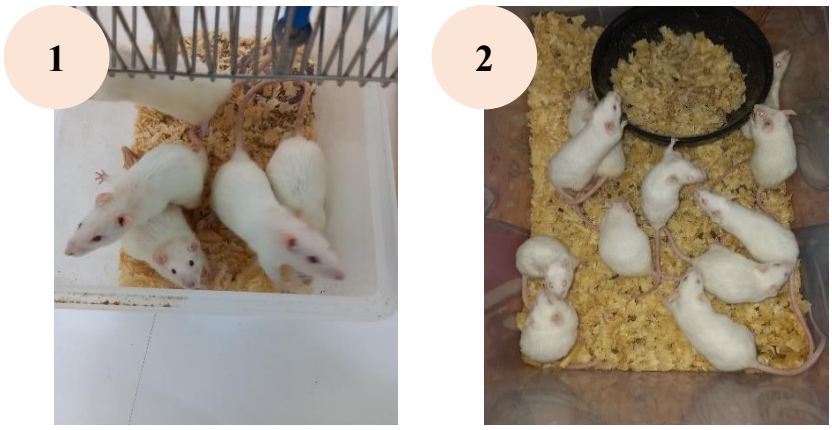

Figure 8: Wistar rats were used for wound healing evaluation **(1)**, Albino mice membrane permeability assay evaluation **(2)**

II.1.2. Non-biological material

The table 3 below comprehensively lists all materials required for the experimental procedures. certain specific protocol details are provided in the annex1 for further clarity.

Table 3: Classification of non-biological materials used in experimental protocols

Chemical reagents	Laboratory equipment	Other items
Silver nitrate ($AgNO_3$)	Volumetric flask	Medical adhesive tape
Polymer I	Microtome	Parafilm
Polymer II	Test tube	Syringes
Polymer III	UV-vis spectrophotometer	Tweezers
Plasticizer	Ball mill	Scalpel
Paracetamol 1% IV	Micropipette	Scissors
Sodium hydroxide (NaOH)	Glass Petri dish	Cotton
Potassium hydroxide (KOH)	Thermometer	
Monopotassium phosphate	Zetasizer	
Ether	Heating magnetic stirrer	
Propofol 1% (anesthetic)	Analytical balance	
Chloroform	Homogenizer	
Formaldehyde 10%	Vortex mixer	
Physiological saline solution	Sonication probe	
Paraffin	Optical microscope	

II.2. Methods

II.2.1. Synthesis of silver nanoparticles

Silver nanoparticles were synthesized using the mechanical milling (ball milling) technique. A total of 1.5 g of silver nitrate was mixed with 10 g of polymer I, maintaining a mass ratio of 1.5:10 ($AgNO_3$: Polymer I). The mixture was placed in a planetary ball mill (agate milling jar and agate grinding ball). The system was sealed with its lid and operated in cycles of milling followed by a pause, to prevent overheating. After a total milling time of 12 hours and 30 minutes, the process was stopped. The resulting powder was collected and stored in a hermetically sealed, light-protected container for further analysis.

II.2.2. Characterization of silver nanoparticles

a) UV-Visible spectroscopy

To confirm the formation and estimate the optical properties of AgNPs, UV-Vis spectroscopy was performed. An aliquot of 0.03 g of the synthesized sample was dispersed in 10 mL of distilled water and homogenized using a vortex mixer to ensure uniform distribution. The solution was then transferred into a quartz cuvette. The UV-Vis absorption spectrum was recorded over the range of 300 - 600 nm.

b) Dynamic Light Scattering (DLS) and Zeta Potential

For particle size distribution and surface charge analysis, DLS and zeta potential measurements were conducted. A sample of 0.1 g of the synthesized powder was dispersed in 30 mL of distilled water and sonicated using a sonication probe to ensure proper dispersion. The homogenized solution was then filtered using a 0.45 µm microfilter to remove any contaminants. The resulting filtrate was analyzed using a Zetasizer to assess nanoparticles size and surface stability.

II.2.3. Formulation protocol of transdermic polymer-based system incorporating silver nanoparticles

The formulation process consisted of preparing a polymer-based hydrogel, incorporating silver nanoparticles, and casting the final mixture into films for transdermic use for wound healing evaluation. The quantities of the components used are detailed in **Table 4**

Table 4: Composition of the silver nanoparticles–loaded biofilm formulation

Component	Concentration range (% w/w)
Polymer II	0.5 – 2.0
Polymer III	1.0 – 4.0
Plasticizing Agent	0.5 – 1.5
Silver Nanoparticles (AgNPs)	< 1.0
Distilled Water	q.s.p. to 100

II.2.3.1. Polymer II-based hydrogel preparation

Before proceeding with the formulation steps, it is important to note that the polymer II-based hydrogel was prepared using a standard method. Once the gel was formed and homogenized, it was stored in a refrigerator overnight to stabilize the structure and dissipate air bubbles, an essential process for stabilizing the hydrogel structure and optimizing its physicochemical properties. The next day, the hydrogel was filtered using a fine mesh strainer to remove any undesirable debris.

II.2.3.2. Polymer III-based hydrogel preparation

Separately, an amount of polymer III was dissolved in 10 mL of distilled water and heated in a water bath at 60°C under constant stirring until a homogeneous hydrogel was obtained.

II.2.3.3. Preparation of AgNPs dispersion

To prepare the silver nanoparticles dispersion, an amount of AgNPs powder was mixed into 30 mL of distilled water and sonicated using an ultrasonic probe to ensure uniform dispersion.

II.2.3.4. Final biofilm formulation

In a water bath at 80 °C, the polymer II-based hydrogel was stirred using a magnetic stirrer. The polymer III-based hydrogel, the plasticizer, and the AgNPs dispersion were added sequentially to the preparation. The mixture was stirred thoroughly until a homogenous blend was achieved.

II.2.3.5. Casting and drying of biofilms

As presented in figure 9, the final biofilm-forming solution was poured into glass Petri dishes and evenly spread across the surface. The dishes were then incubated in a laboratory oven at 60°C for 20 hours.

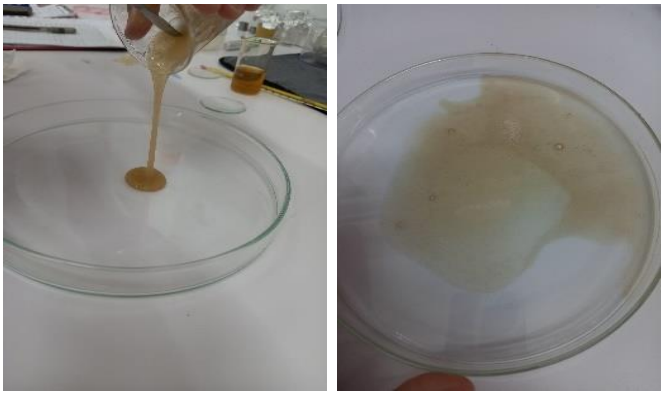

Figure 9: Casting and drying of the film

II.2.3.6. Transdermal patches formation and conditioning

After drying, the formed biofilms were carefully removed using tweezers, and circular discs of 20 mm diameter were cut using a circular mold. The individual pieces of biofilm were placed onto adhesive medical bandages (Sparadrap), sealed, and stored using cling film for further use in the wound healing studies. The figure 10 exhibits these different steps.

Figure 10: Preparation and conditioning of biofilm-based bandage discs for wound healing applications

II.2.4. Membrane permeability assays (Ex vivo)

The ex vivo permeability study was carried out to evaluate the diffusion of silver nanoparticles from the formulated biofilm across excised mouse skin, using a Franz diffusion cell apparatus showed in figure 11.

Figure 11: Franz diffusion cell apparatus

- **Experimental Protocol**

The preparation of the phosphate buffer used in this study was carried out according to standard procedures and is described in detail in **Appendix 1**

1) Preparation of the Skin Sample

A laboratory mouse was sacrificed using chloroform inhalation, by ethical guidelines. The dorsal side skin was excised using sterile surgical instruments, and the underlying subcutaneous fat was carefully removed. The skin was rinsed with phosphate buffer solution to eliminate any remaining biological residues, then allowed to equilibrate at room temperature before use in the diffusion experiment. These steps are illustrated in figure 12.

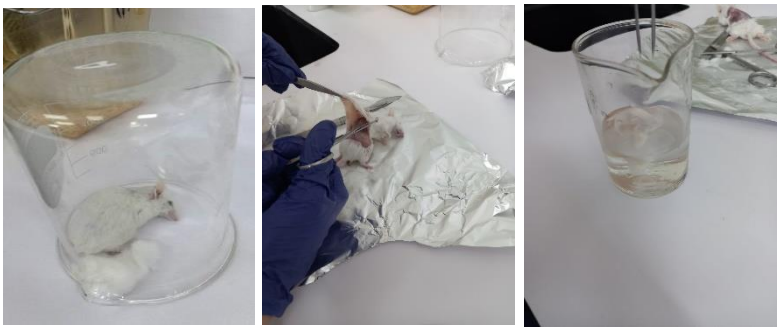

Figure 12: Protocol for excised mouse skin preparation

2) Assembly of the Franz Diffusion Cell

The receptor compartment of the Franz diffusion cell was filled with the phosphate buffer, and a magnetic stir bar was placed inside to ensure continuous agitation. The prepared skin was mounted between the donor and receptor compartments, with the stratum corneum facing the donor side. The tested AgNPs-based transdermic patch, was applied to the donor compartment. The system was then sealed using plastic clamps to avoid leakage. The entire setup was maintained under constant stirring at the temperature maintained at 37 °C through a thermostatically controlled system. The assembly steps are exhibited in figure 13.

Figure 13: Stepwise assembly of the Franz cell diffusion

3) Sampling and spectrophotometric analysis

Samples of 2.5 mL were withdrawn from the receptor compartment at 60-minute intervals. Each sample was immediately analyzed using UV-Visible spectrophotometry at 427 nm, corresponding to silver nanoparticles' characteristic surface plasmon resonance peak. Following each sampling, the withdrawn volume was replaced with an equal volume of freshly prepared buffer solution maintained at 37 °C to preserve sink conditions throughout the experiment. The sampling process continued until the permeation profile reached a plateau, indicating saturation and the end of effective diffusion.

II.2.5. Assessment of the Wound Healing Potential of the AgNPs-based transdermic patch

1. Objective of the study

This study aims to evaluate the wound healing efficacy of a biofilm containing silver nanoparticles on experimentally induced excisional wounds in laboratory rats. The circular excision wound model was selected for its reproducibility and suitability for quantitative wound measurement. This model allows for continuous observation of the healing process until wound closure.

2. Principle of the method

The principle consists of inducing full-thickness skin wounds via circular excision (8 mm diameter) on the right flank of each rat. The wounds are then treated daily with either the test formulation, a reference commercial ointment, or left untreated as a control. Wound progression is monitored macroscopically and quantitatively assessed through planimetry and histological evaluation over 21 days.

3. Animal grouping

A total of 22 female albino rats were used, divided into three experimental groups as shown in Table 5. On the day of the experiment, rats were marked on their tails and randomly assigned to one of the three groups mentioned above.

Table 5: Experimental grouping of animals for in vivo evaluation

Group	Number of rats	Treatment description
Control (T)	8	No treatment applied
Test (E)	8	Wound treated with transdermic AgNPs-based patches
Reference (R)	6	Wound treated with commercial healing ointment (Cicatryl®)

4. Wound induction procedure

Rats are anesthetized via intraperitoneal injection of propofol. The anesthetic dosage of 75 mg/kg was used for calculating the injection volumes for Propofol 1% (10 mg/mL concentration). Each rat's required dose in milligrams was computed based on its body weight (equation 1), followed by conversion into milliliters using the drug concentration (equation 2).

The computed values of injected anesthesia volumes are presented in appendix 2.

$$Dose\ (mg) = \frac{75 * weight\ (g)}{1000} \qquad (1)$$

$$Injection\ volume\ (mL) = \frac{Dose\ (mg)}{10} \qquad (2)$$

The right flank area is shaved using scissors to expose the skin, then the exposed skin is disinfected with 70% surgical alcohol.

• Wound Creation

Each rat was placed in a stable position on the dissection table. A circular area measuring 8 mm in diameter was marked on the right flank using a sterile cylindrical ruler. While under anesthesia, the marked skin was carefully excised using sterile scissors and forceps to create a full-thickness wound, exposing the underlying tissue. The wound area was then gently cleansed with sterile gauze soaked in 0.9% physiological saline to ensure clear visibility and accurate assessment of the wound surface. To minimize postoperative pain, 1 mL of a 1% paracetamol solution was administered intraperitoneally immediately after wound creation.

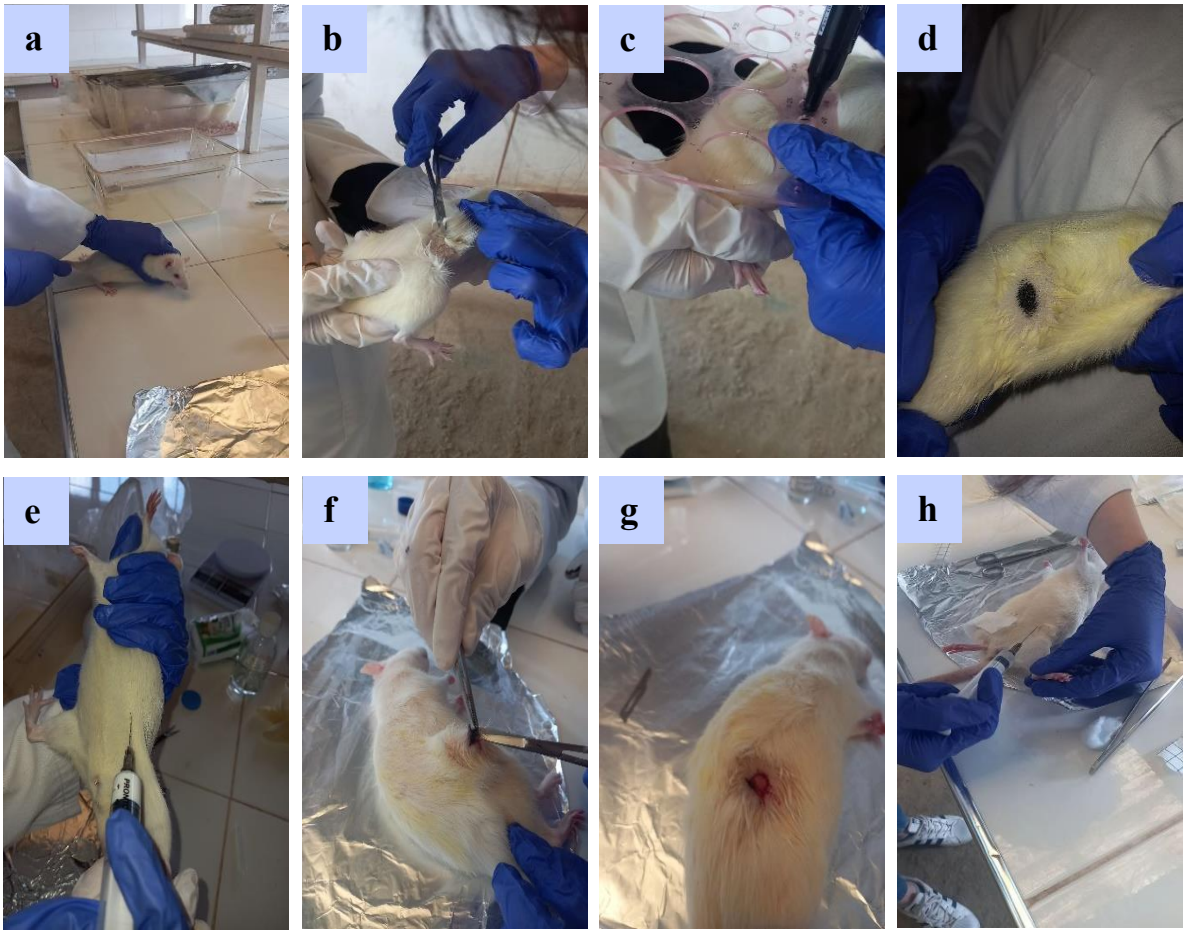

Figure 14: Wound induction procedure. **(a)** Animal restraint, **(b)** Hair removal, **(c, d)** Skin marking on the right flank, **(e)** Anesthesia induction (Propofol 1%), **(f, g)** Skin excision, **(h)** Analgesic injection (Paracetamol 1%)

5. Treatment application

Treatments are applied topically once daily starting from day 0 (J0) for Groups (R) /(E) until complete re-epithelialization, but the control group will not receive any treatment. Wound surface impressions were taken on days 0, 5, 10, 15, and 21, following the sacrifice of rats in each group at the respective time points.

6. Expression of results

The wound surface areas were calculated using **ImageJ** software. The percentage of wound surface area reduction, both for untreated wounds, wounds treated with the reference product **Cicatryl®,** and those treated with the transdermic AgNP**s-based patches**, was determined using the formula (3).

$$Wound\ area\ reduction\ (\%) = (wound\ area\ on\ day\ 0 - wound\ area\ on\ day\ n) * 100 \quad (3)$$

II.2.6. Histopathological technique

Histopathology enables the microscopic examination of biological tissues, providing essential insights into cellular architecture and pathological alterations. In this study, the procedure was applied exclusively to rat skin tissue samples. The steps followed are outlined below.

1. **Macroscopic examination**

Skin samples were carefully examined with the naked eye to evaluate general features such as the presence of visible lesions. Tissue fragments were placed into pre-labeled histological cassettes and fixed in 10% buffered formalin.

2. **Tissue processing**

The fixed samples underwent dehydration in an automated tissue processor for 14 hours using ascending alcohol concentrations (70%, 90%, 96%, and 100%), followed by xylene clearing. Tissues were then embedded in paraffin to prepare blocks for sectioning.

3. **Microtomy**

Paraffin blocks were sectioned at a thickness of 3 µm using a microtome. The ribbons were gently floated on a 37 °C water bath to remove folds and then mounted on labeled glass slides.

4. **Staining**

Tissue sections were deparaffinized, rehydrated through decreasing alcohol grades, and stained using a standard trichrome method. Slides were then dried in an oven at 58 °C for 10 minutes to fix the stain.

5. **Mounting**

A mounting medium and xylene were used to apply coverslips over the stained tissue, ensuring bubble-free adhesion and long-term preservation.

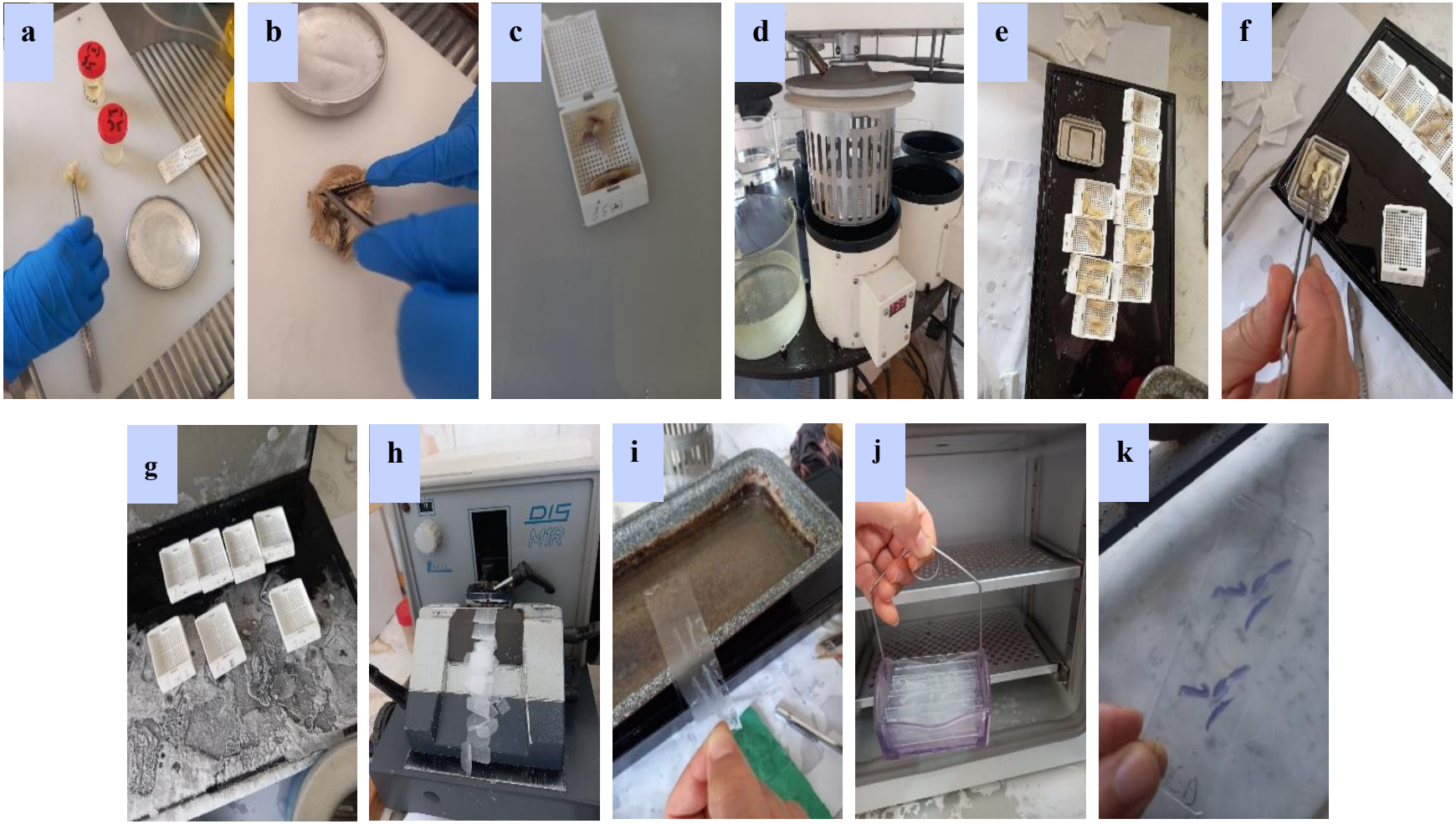

Figure 15: Steps of the histological study. **(a)** Tissue fixation in Formalin 10%, **(b)** macroscopic trimming, **(c)** placement into cassettes, **(d)** Automated tissue processing, **(e, f)** Paraffin embedding, **(g)** Block cooling, **(h)** Microtomy, **(i)** Floatation and slide mounting, **(j)** Slide drying, **(k)** Straining for microscopic examination

Chapter III:
Results and Discussion

Chapter III: Results and Discussion

III.1. Results

III.1.1. Synthesis of silver nanoparticles

III.1.1.1. Characterization via color change observation

When polymer I and $AgNO_3$ were mixed, the initially white powder gradually turned yellow during the milling process. This color change indicates the formation of silver nanoparticles through solvent-free synthesis, confirming the success of the process, as shown in figure 16.

Figure 16: Visual observation of AgNPs formation via color change

III.1.1.2. UV-Visible Spectroscopy

The UV-Vis spectrum (Figure 17) displays a strong and well-defined surface plasmon resonance (SPR) peak at 427 nm. This peak confirms the formation of silver nanoparticles, as it corresponds to the characteristic SPR band of spherical AgNPs. Silver nanoparticles exhibit a Surface Plasmon Resonance phenomenon when exposed to light, which typically appears between 400–450 nm for silver, depending on the size, shape, and environment of the nanoparticles.

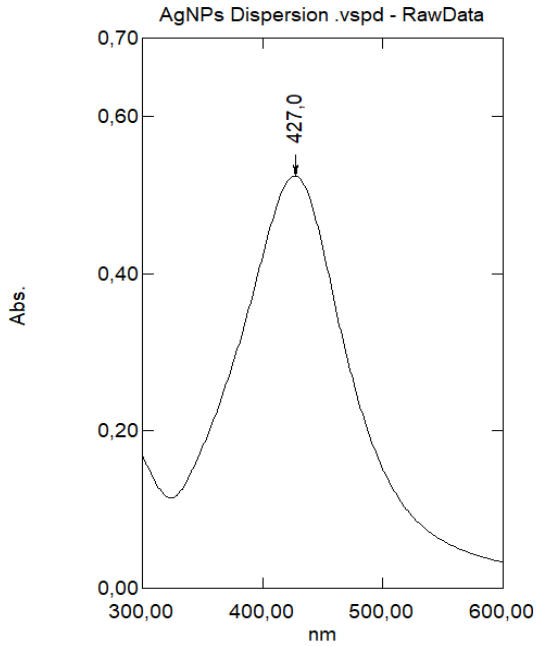

Figure 17: UV-vis spectrum of the synthesized AgNPs

III.1.1.3. Dynamic Light Scattering (DLS)

The hydrodynamic diameter of the synthesized silver nanoparticles was measured using Dynamic Light Scattering, and the size distribution graph is presented in Figure 18.

The average particle size was found to be approximately 77.5 nm, indicating a bimodal distribution. Specifically, the analysis revealed two distinct populations: the first with a mean diameter of 106.4 nm (88.1% intensity) and the second with a smaller diameter of 19.57 nm (11.9% intensity). The presence of a bimodal size distribution may have important implications for the antimicrobial activity of AgNPs.

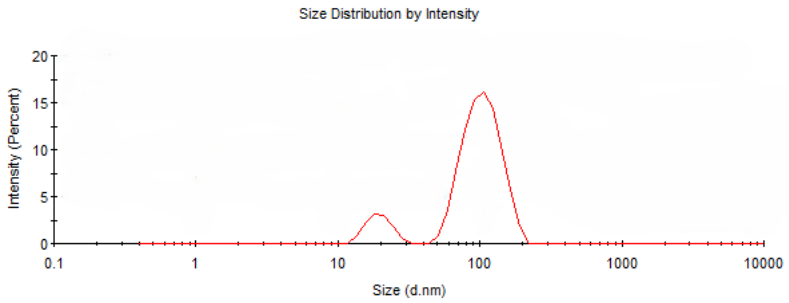

Figure 18: Size distribution of the synthesized AgNPs

III.1.1.4. Zeta Potential

Zeta potential is a critical parameter that reflects the surface charge of nanoparticles and directly influences their colloidal stability. The zeta potential of the synthesized AgNPs was measured to be -6.79 mV, as shown in Figure 19. While this value falls within the generally accepted range of stability (±30 mV), it indicates moderate electrostatic repulsion between particles, which helps prevent aggregation in aqueous media.

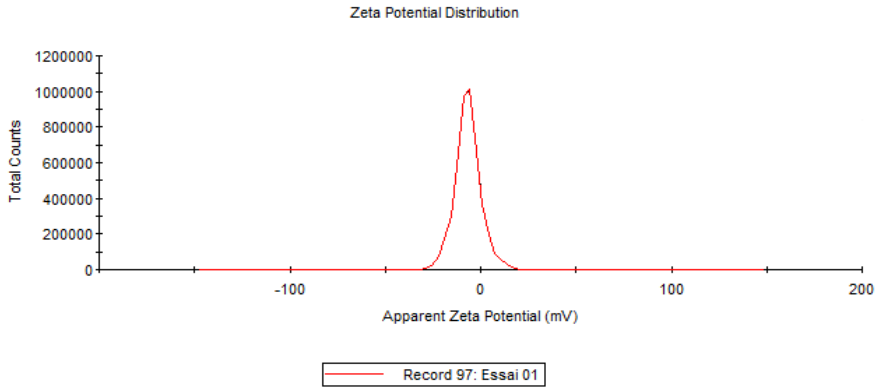

Figure 19: Zeta potential distribution of synthesized silver nanoparticles

III.1.2. Spectrophotometric analysis of membrane permeability assays (Ex vivo)

As part of the wound healing strategy, a polymer-based transdermal patch containing silver nanoparticles was formulated to enable controlled release through the skin. This system was evaluated using an ex vivo permeability assay to assess its ability to deliver AgNPs across the skin barrier. The physical appearance and structural integrity of the patches were also visually assessed in Figure 20.

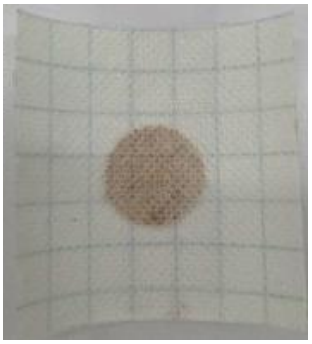

Figure 20: Polymer-based transdermal patch containing silver nanoparticles

The graph titled "Cumulative permeation of AgNPs over time", obtained by UV-Visible spectrophotometry at 427 nm and shown in figure 21, illustrates the gradual diffusion of silver nanoparticles through the skin. Following an initial latency phase, a steady permeation is observed up to 12 hours, after which a plateau phase indicates the establishment of a diffusion equilibrium. This profile reflects controlled release kinetics, confirming the ability of AgNPs to sustainably penetrate the skin barrier.

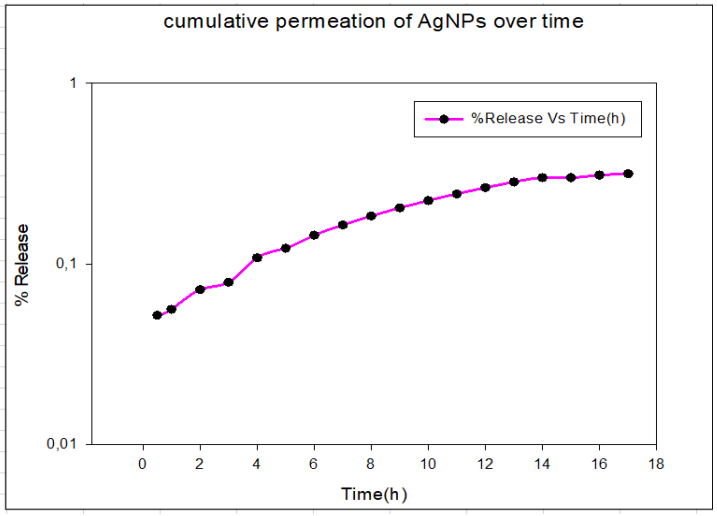

Figure 21: Cumulative ex vivo permeation profile of silver nanoparticles measured by UV-visible

III.1.3 Histological study of the wound healing process

III.1.3.1. Macroscopic healing

The progression of wound healing in rats was monitored through macroscopic observation and photographic documentation, as shown in Figure 22 below.

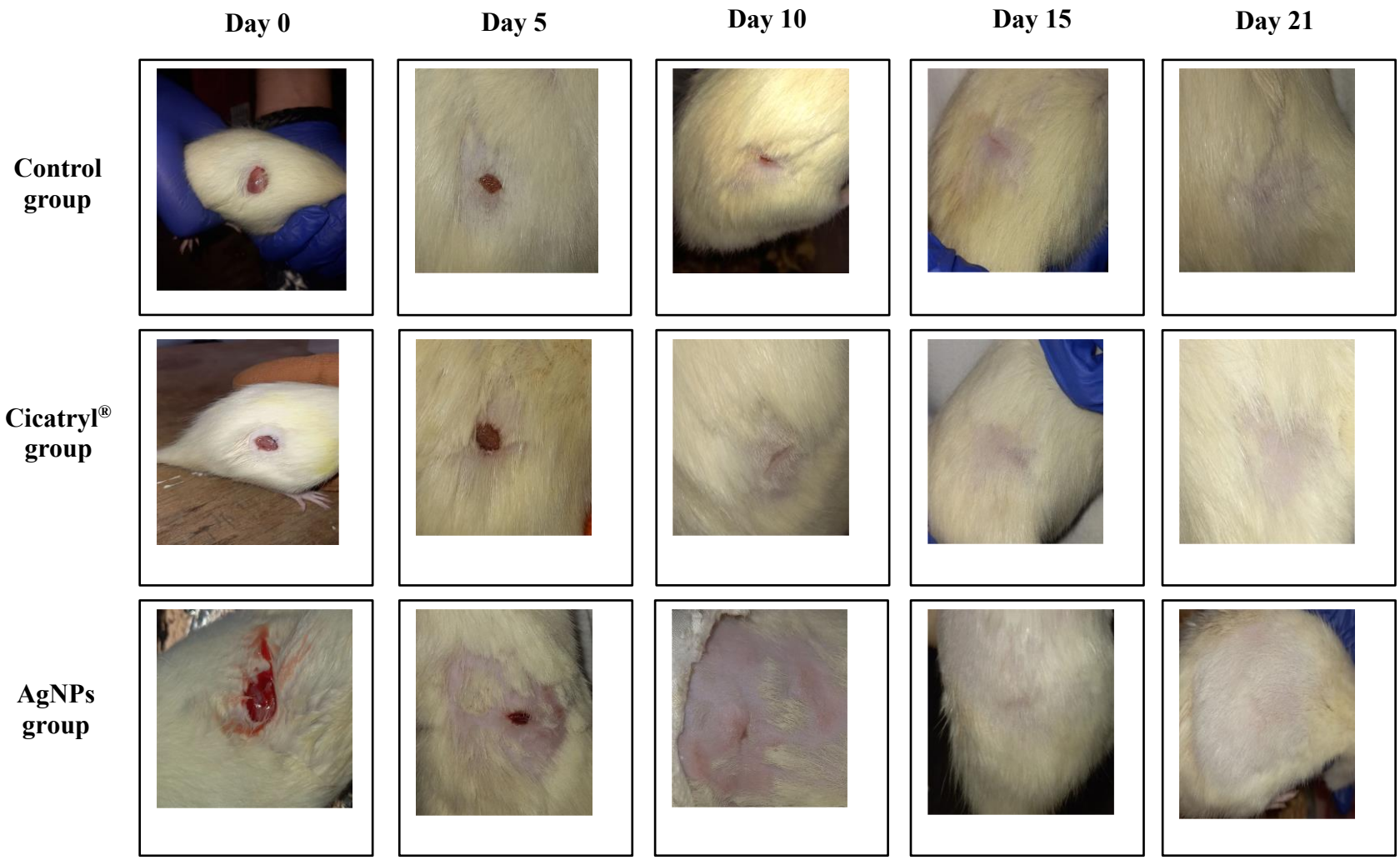

Figure 22: Macroscopic appearance of wounds at day 0, 5, 15 and 21 for the three experimental groups

III.1.3.2. Expression of Results

The wound surface area (mm^2), calculated from photographic images using ImageJ software, is presented in Table 6. The corresponding percentage reduction in wound area for each group is shown in Table 7.

The transdermal AgNPs-based patches treated group demonstrated a significantly faster wound healing response compared to both control and reference groups. By day 5, wounds treated with silver nanoparticle patches exhibited nearly 90% surface area reduction, and over 99% by day 15. In contrast, the control and Cicatryl® groups showed slower healing, with the control group lagging behind throughout the study period. These findings suggest that AgNPs based treatment markedly enhances wound contraction and accelerates the healing process.

Table 6: Wound surface area (mm^2) measured over time for control, reference (Cicatryl®), and AgNPs-based patches treated groups

Day	Control group (mm^2)	Reference group Cicatryl® (mm^2)	AgNPs-treated group (mm^2)
Day 0	665.73	665.73	665.73
Day 5	304.27	190.96	69.98
Day 10	86.04	164.79	53.46
Day 15	33.18	50.73	3.77
Day 21	0	0	0

Table 7: Percentage of wound surface area reduction over time in control, reference (Cicatryl®), and AgNPs-based patches treated groups

Day	Control group reduction (%)	Reference group Cicatryl® reduction (%)	AgNPs-treated group reduction (%)
Day 0	0	0	0
Day 5	54.29	71.31	89.49
Day 10	87.08	75.25	91.97
Day 15	95.02	92.38	99.43
Day 21	100	100	100

III.1.3.3. Microscopic healing

Histological examination of skin tissue sections stained with trichrome enabled the evaluation of the wound healing process over the 21-day observation period in the control, reference (Cicatryl®), and AgNPs-treated groups of Wistar rats.

- **The skin of the control group**

Histological analysis of the control group revealed a delayed and suboptimal wound healing process. At day 5, the tissue showed pronounced inflammatory infiltration, immature granulation tissue, and absent or partial re-epithelialization. By Day 21, there was partial epidermal regeneration with persistent fibrotic zones and limited reappearance of skin appendages. These findings are consistent with a normal, untreated healing response characterized by prolonged inflammation and incomplete tissue remodeling, and limited reappearance of skin adnexal structures, such as sweat glands and a few hair follicles.

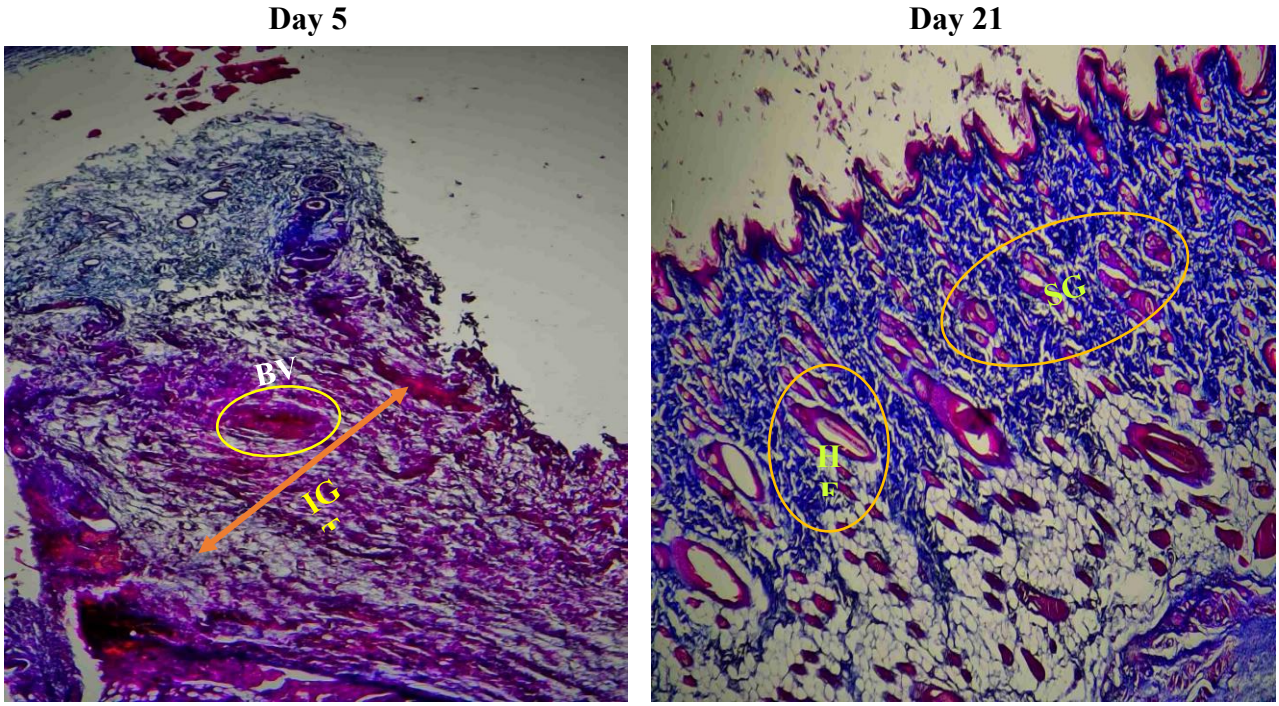

Figure 23: Histology of skin from the control group on days 5 and 21 (Trichrome staining, x4)
IGT: Inflammatory Granulation Tissue, **HF**: Hair Follicle, **SG**: Sweat Glands, **BV**: Blood Vessel

➢ **The skin of the reference (Cicatryl®) group**

The reference group treated with Cicatryl® cream showed enhanced wound healing compared to the control. On day 5, there was visible granulation tissue with moderate inflammation, new blood vessels, and early re-epithelialization at the wound edges. Collagen fibers were already present but appeared thin and loosely arranged, showing the beginning of tissue repair.

By day 21, the wound was almost fully healed, with a complete epidermal layer, dense and well-organized collagen bundles, and very few inflammatory cells. The dermis showed signs of remodeling and regeneration of skin structures with the initial reappearance of skin adnexal structures. These results suggest that Cicatryl® effectively accelerates both epidermal regeneration and collagen remodeling.

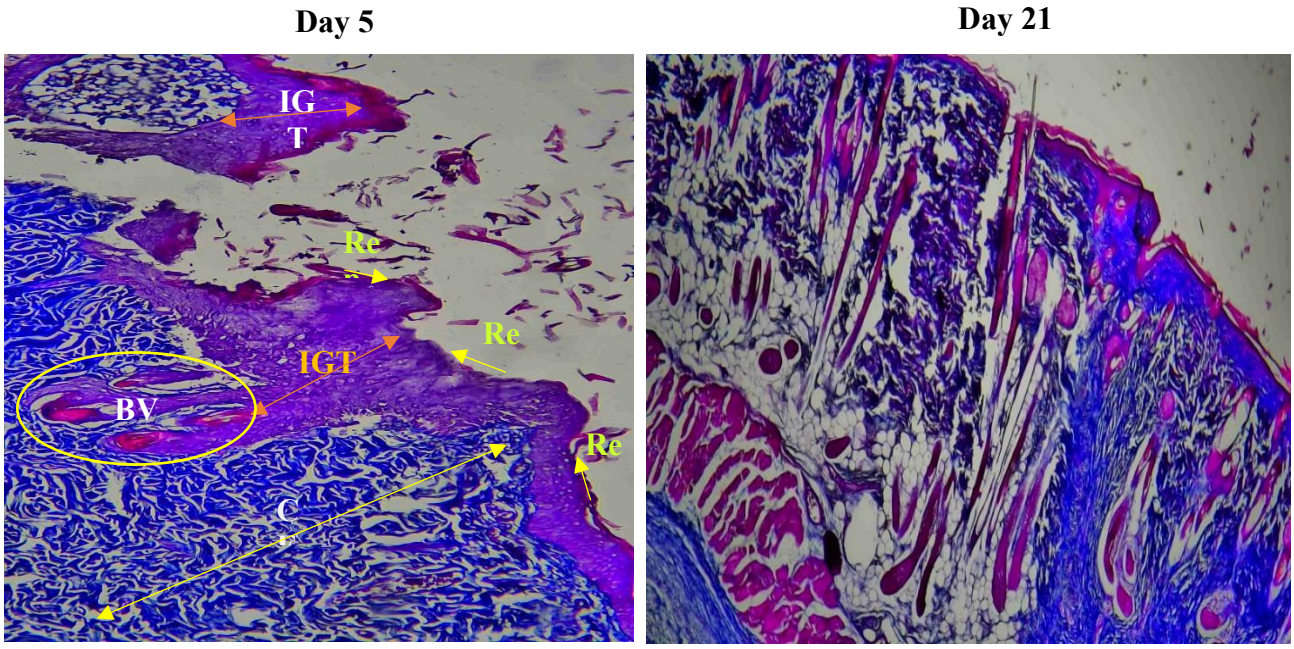

Figure 24: Histology of skin from the reference group treated with Cicatryl® (Trichrome staining) on day 5 (x4) and day 21 (x10)
IGT: Inflammatory Granulation Tissue; **Rep:** re-epithelialization; **CF:** Collagen Fibers; **BV:** Blood Vessels

- **The skin of the transdermal AgNPs-based treated group**

The AgNPs-treated group exhibited a markedly highly active inflammatory response on day 5, characterized by dense infiltration of immune cells, extensive granulation tissue formation, and early evidence of angiogenesis. Compared to other groups, this inflammatory phase appeared significantly more intense, reflecting the strong immunostimulatory properties of silver nanoparticles. Such heightened inflammation is essential for effective wound debridement, microbial clearance, and initiation of the regenerative process.

By day 21, inflammation had substantially resolved, with the tissue showing complete re-epithelialization, well-organized collagen fibers, and clear signs of dermal remodeling. Notably, sebaceous glands, absent in the other groups, reappeared in this group, along with hair follicles, indicating advanced structural and functional skin regeneration. This progression from a robust early immune response to complete tissue repair underscores the dual role of AgNPs in modulating inflammation and promoting effective wound healing.

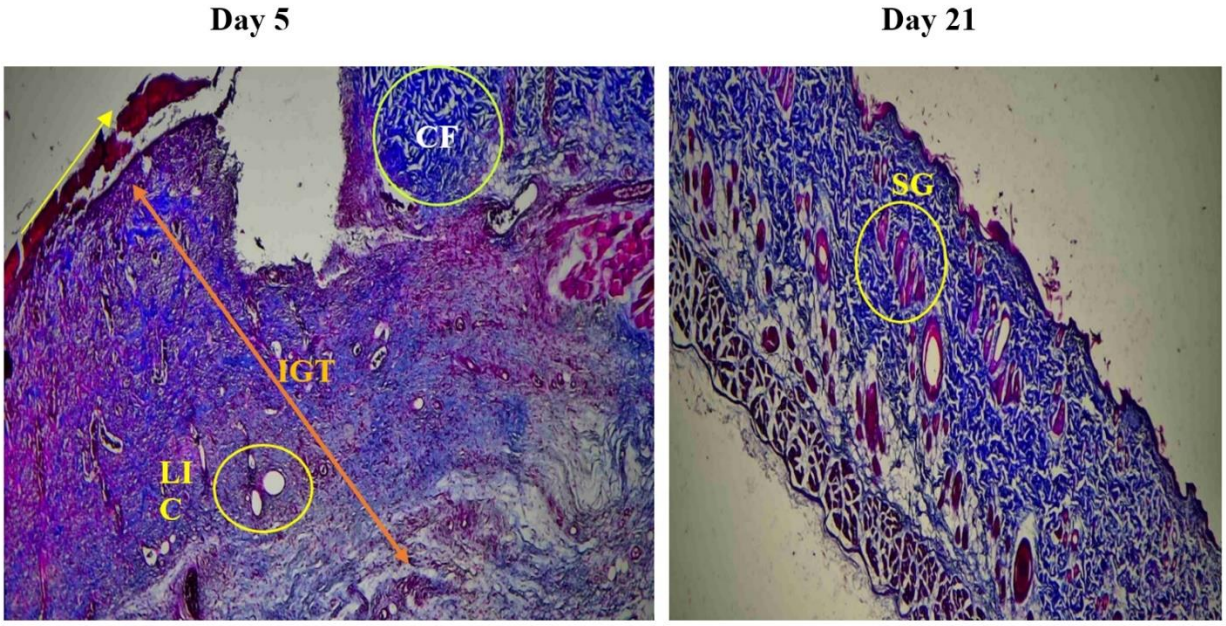

Figure 25: Histology of skin in the AgNPs-treated group (Trichrome staining, x4) on days 5 and 21
LIC: Large Immune Cell; **IGT:** Inflammatory Granulation Tissue; **CF:** Collagen Fibers; **SG:** Sebaceous Glands

III.2. Discussion

III.2.1. Characterization via color change observation

The observed color change from white to yellow-brown following the mixing of polymer I and $AgNO_3$ provides a reliable visual indication of silver nanoparticles formation. This transformation is attributed to the excitation of surface plasmon resonance (SPR), a phenomenon commonly observed in AgNPs synthesis (**Sharma V. K., et al., 2009**).

The yellow to brown hue is characteristic of nanoscale silver due to its interaction with visible light, and this change in color has been widely reported as a primary qualitative marker of successful silver nanoparticles synthesis (**Neto W. P., et al., 2023**).

Zhang X. F., et al., (2016) reported that the synthesis of silver nanoparticles typically follows a multistep mechanism involving reduction, nucleation, growth, and stabilization. In the initial stage, silver ions (Ag^+) are reduced to elemental silver (Ag^0) through the action of a chemical or biological reducing agent. Once reduced, the silver atoms begin to aggregate into small clusters through a process known as nucleation, which marks the formation of the nanoparticle core. As additional silver atoms accumulate, these clusters grow and develop into stable nanoparticles. To prevent aggregation and ensure colloidal stability, capping agents such as polymers or biomolecules are introduced, providing steric or electrostatic stabilization.

III.2.2. UV-Visible Spectroscopy

Singh S., et al., (2015) observed a peak at 427 nm when using maltose as a reducing agent and PVP as a stabilizer strongly supporting the reliability of the observed SPR signal in this study. Polymers play a critical role as a capping agent, providing steric stabilization by forming a protective polymer layer around the AgNPs, which preserves their optical properties and prevents particle clustering (**Wang Z. L., et al., 2005**).

Gu H., et al. (2012) reported that silver nanoparticles synthesized exhibited a strong SPR peak in the 420-430 nm range, validating our spectrophotometric results and confirming the successful formation of well-dispersed AgNPs.

III.2.3. Dynamic Light Scattering

The wound healing process involves a coordinated sequence of events, hemostasis, inflammation, proliferation, and remodeling, where immune regulation, microbial control, and tissue regeneration are essential. In this context, the physicochemical properties of silver nanoparticles, particularly particle size and distribution, play a crucial role in determining their biological behavior and therapeutic potential. The DLS analysis in this study revealed a bimodal size distribution with a polydispersity index (PDI) below 0.3, indicating a relatively uniform and stable colloidal system.

Smaller AgNPs, due to their high surface-area-to-volume ratio, exhibit enhanced reactivity and efficient interaction with bacterial membranes, promoting membrane disruption and reactive oxygen species generation (**Marambio-Jones C., et al., 2010**). These effects are particularly beneficial during the inflammatory phase, where antimicrobial activity is vital to prevent infection and support a clean wound bed. According to **Buzea C., et al., (2007**), nanoparticle aggregates can further facilitate pore formation in cell membranes, allowing for deeper penetration and sustained cytotoxic effects.

Meanwhile, the larger particles in the second population may act as a reservoir of silver ions, remaining on the wound surface to provide long-lasting antimicrobial protection. This dual behavior, rapid action from smaller particles and sustained release from larger ones, may enhance therapeutic outcomes. Moreover, the good particle size distribution confirmed by the PDI value supports consistent bioavailability, which is essential for AgNPs to interact effectively with fibroblasts and keratinocytes, promoting epithelial regeneration and extracellular matrix remodeling (**Rigo C., et al., 2013**).

III.2.4. Zeta Potential

Nanoparticles with a zeta potential between -10 mV and +10 mV are typically considered near-neutral and may show limited long-term colloidal stability. However, in this study, the observed negative surface charge, although modest, is likely sufficient to ensure short-term dispersion stability due to electrostatic repulsive forces **(Bhattacharjee S., 2016).**

Overall, the measured physicochemical characteristics suggest that the synthesized AgNPs possess adequate properties for biological interaction, including effective membrane penetration, moderate colloidal stability, and a favorable size distribution for antimicrobial applications.

III.2.5. Spectrophotometric analysis of membrane permeability assay (ex vivo)

The permeation profile in our experiment aligns with the findings of **Larese Filon F., et al., (2009),** who observed that silver penetration is time-dependent and enhanced by prolonged exposure, with detectable amounts accumulating in both the epidermis and dermis. Moreover, the moderate slope of our release curve suggests a controlled and sustained release, a desirable characteristic for topical wound applications, as it ensures a continuous presence without systemic toxicity.

III.2.6. Histological study of the wound healing process

The wound surface area data in our study are consistent with results reported by **Ahamed M., et al., (2022)**, who observed ~85-90% wound contraction in rats treated with AgNPs-based formulations by day 14, reaching near-complete closure by day 21. Our results suggest an even more rapid wound healing trajectory, likely due to the synergistic effects of nanoparticles size, used polymers, and local anti-inflammatory action. This is further supported by our histological data, which revealed earlier epithelial regeneration and better-organized collagen matrix in transdermal AgNPs- based patches treated wounds.

These findings align with other researches. **Singh P., et al. (2022),** in a rat wound model, reported accelerated healing, characterized by improved tensile strength and reduced inflammation. Similarly, **Cheng L., et al. (2024)** observed a significant increase in wound contraction in excisional wounds treated with AgNPs-based formulations, further substantiating the effectiveness of silver nanoparticles in promoting wound closure.

Overall, our results contribute to the growing body of evidence indicating that well-formulated AgNPs systems, particularly those with optimized particle size and polymer-based support, can markedly enhance wound healing outcomes, both at the macroscopic (surface contraction) and microscopic (tissue organization) levels.

Conclusion and perspectives

Conclusion and perspectives

In this work, we developed and evaluated a simple yet effective method for the synthesis of silver nanoparticles, with the primary objective of formulating a transdermal AgNPs-based patches capable of promoting skin regeneration. The synthesized nanoparticles were successfully characterized using multiple physicochemical techniques, confirming their formation, nanoscale size, stability, and surface properties parameters essential for biomedical applications.

From a biological perspective, the AgNPs-embedded biofilm demonstrated notable wound healing activity in vivo. The results indicated accelerated tissue repair, reduced inflammation, and improved dermal remodeling, all of which underscore the therapeutic efficacy of the formulation. In addition, histopathological analyses revealed more complete re-epithelialization and restoration of skin architecture in AgNPs-treated group compared to control and reference.

These ex vivo studies revealed that permeation of AgNPs profile reflected a sustained release kinetic, confirming the formulation's ability to deliver active agents in a controlled and continuous manner a desirable property for wound care products aimed at reducing dressing frequency and enhancing healing outcomes.

Together, these findings validate the relevance of AgNPs-based systems as innovative therapeutic tools for wound management, with the dual advantage of promoting healing.

To build upon the outcomes of this study and facilitate translational applications, several future perspectives may be explored. These include:

- Evaluation of mechanical and physicochemical properties of the prepared biofilm,
- Evaluation of the antimicrobial activity of the developed transdermal patches,
- Evaluation of long-term safety and systemic absorption,
- Clinical testing in human models,
- Incorporation of AgNPs into multifunctional hybrid systems with anti-scarring or analgesic properties.

Bibliographic References

Bibliographic & References

- Ahamed, M., Akhtar, M. J., & Alhadlaq, H. A. (2022). Silver Nanoparticles-Based Therapeutics for Efficient Wound Healing: A Review. Pharmaceuticals, 15(1), 194.
- Ahmed, S., Ahmad, M., Swami, B. L., & Ikram, S. (2016). A review on plant extract-mediated synthesis of silver nanoparticles for antimicrobial applications: A green expertise. *Journal of Advanced Research, 7*(1), 17–28. https://doi.org/10.1016/j.jare.2015.02.007
- Alexander, J. W. (2009). History of the medical use of silver. *Surgical Infections, 10*(3), 289–292. https://doi.org/10.1089/sur.2008.9941
- Barhoumi, T., Bouchareb, R., Alroqi, F., Nefzi, A., & colleagues. (2025). Inflammaging and immunosenescence: Role in aging-associated cardiovascular
- Bayda, S., Adeel, M., Tuccinardi, T., Cordani, M., & Rizzolio, F. (2019). The history of nanoscience and nanotechnology: From chemical–physical applications to nanomedicine. *Molecules, 25*(1), 112. https://doi.org/10.3390/molecules25010112
- Benedetti, J. (n.d.). 2024.Structure and function of the skin. In *Skin Disorders – Merck Manuals*.https://www.merckmanuals.com/home/skin-disorders/biology-of-the-skin/structure-and-function-of-the-skin
- Bhattacharjee, S. (2016). DLS and zeta potential – What they are and what they are not? *Journal of Controlled Release, 235*, 337–351.
- Bhushan, B. (2017). Introduction to nanotechnology. In *Springer handbook of nanotechnology* (pp. 1–19). Springer. https://doi.org/10.1007/978-3-662-54357-3_1
- Buzea, C., Pacheco, I. I., & Robbie, K. (2007). Nanomaterials and nanoparticles: Sources and toxicity. *Biointerphases, 2*(4), MR17–MR71.
- Cheng L, Zhang S, Zhang Q, Gao W, Mu S, Wang B. Wound healing potential of silver nanoparticles from Hybanthus enneaspermus on rats. Heliyon. 2024 Aug 10;10(17):e36118. doi: 10.1016/j.heliyon.2024.e36118. PMID: 39286104; PMCID: PMC11403429.
- Cleveland Clinic. (2023). *Skin: Layers, structure and function*. Cleveland Clinic. https://my.clevelandclinic.org/health/articles/10978-skin

- Duman, H., Aygün, A., Bozkurt, A. G., & Gündüz, M. (2024). Characterization and evaluation of green-synthesized silver nanoparticles using novel biological sources. Materials Science for Energy Technologies, 7, 34–42.
- Duman, H., Eker, F., Akdaşçi, E., Witkowska, A. M., Bechelany, M., & Karav, S. (2024). Silver nanoparticles: A comprehensive review of synthesis methods and chemical and physical properties. *Nanomaterials, 14*, 1527. https://doi.org/10.3390/nano14071527
- Eker, F., Duman, H., Akdaşçi, E., Witkowska, A. M., Bechelany, M., & Karav, S. (2024). Silver nanoparticles in therapeutics and beyond: A review of mechanism insights and applications. *Nanomaterials, 14*, 1618. https://doi.org/10.3390/nano14071618
- Elbeshehy, E. K. F., Elazzazy, A. M., & Aggelis, G. (2015). Silver nanoparticles synthesis mediated by new isolates of *Bacillus* spp., nanoparticle characterization and their activity against Bean Yellow Mosaic Virus and human pathogens. *Frontiers in Microbiology, 6*, 453. https://doi.org/10.3389/fmicb.2015.00453
- Franci, G., Falanga, A., Galdiero, S., Palomba, L., Rai, M., Morelli, G., & Galdiero, M. (2015). Silver nanoparticles as potential antibacterial agents. Molecules, 20(5), 8856–8874. https://doi.org/10.3390/molecules20058856
- Gang, X. F., Liu, Z. G., Shen, W., & Gurunathan, S. (2016). Silver nanoparticles: synthesis, characterization, properties, applications, and therapeutic approaches. International Journal of Molecular Sciences, 17(9), 1534. https://doi.org/10.3390/ijms17091534
- Gilaberte, Y., Prieto-Torres, L., Pastushenko, I., & Juarranz, Á. (2016). Anatomy and function of the skin. In *Nanoscience in dermatology* (pp. 1–14). Elsevier. https://doi.org/10.1016/B978-0-12-802926-8.00001-6
- Gu, H., Tian, P., Guo, M., Li, Y., & Hao, X. (2012). Low-temperature electrolytic coloration and spectral properties of sucrose crystals. Spectrochimica Acta Part A: Molecular and Biomolecular Spectroscopy, 91, 269–271. doi:10.1016/j.saa.2012.02.006
- Guo, S., & DiPietro, L. A. (2010). Factors affecting wound healing. Journal of Dental Research, 89(3), 219–229. https://doi.org/10.1177/0022034509359125
- Heather A. Wallace. (2023). Wound Healing Phases - StatPearls - NCBI Bookshelf.
- Ibrahim, H. M. (2015). Green synthesis and characterization of silver nanoparticles using banana peel extract and their antimicrobial activity against representative microorganisms.

Journal of Radiation Research and Applied Sciences, 8(3), 265–275. https://doi.org/10.1016/j.jrras.2015.01.007

- Ita, K. (2020). *Anatomy of the human skin. Transdermal Drug Delivery, 9–18.* doi:10.1016/b978-0-12-822550-9.00002-8
- Jariwala, D., Sangwan, V. K., Lauhon, L. J., Marks, T. J., & Hersam, M. C. (2014). Carbon nanomaterials for electronics, optoelectronics, photovoltaics, and sensing. *Chemical Society Reviews, 42*(7), 2824–2860. https://doi.org/10.1039/C3CS60323K
- Khan, I., Saeed, K., & Khan, I. (2019). Nanoparticles: Properties, applications and toxicities. *Arabian Journal of Chemistry, 12*(7), 908–931. https://doi.org/10.1016/j.arabjc.2017.05.011
- Kolarsick, P. A. J., Kolarsick, M. A., & Goodwin, C. (2006). Anatomy and physiology of the skin. *Journal of the Dermatology Nurses' Association, 1*(1), 30–41.
- Kováčová, M., Daneu, N., Tkáčiková, Ľ., Búreš, R., Dutková, E., Stahorský, M., Bujňáková, Z. L., & Baláž, M. (2020). Sustainable One-Step Solid-State Synthesis of Antibacterially Active Silver Nanoparticles Using Mechanochemistry. Nanomaterials, 10(11), 2119. https://doi.org/10.3390/nano10112119
- Kumar, B., Smita, K., Cumbal, L., & Debut, A. (2014). Green synthesis of silver nanoparticles using Andean blackberry fruit extract. *Saudi Journal of Biological Sciences, 21*(6), 605–609. https://doi.org/10.1016/j.sjbs.2014.07.005
- Lai-Cheong, J. E., & McGrath, J. A. (2013). Structure and function of skin, hair and nails. Medicine, 41(6), 317–320. https://doi.org/10.1016/j.mpmed.2013.04.017
- Lansdown, A. B. G. (2006). Silver in health care: antimicrobial effects and safety in use. Current Problems in Dermatology, 33, 17–34. https://doi.org/10.1159/000093928
- Larese Filon, F., D'Agostin, F., Crosera, M., Adami, G., Bovenzi, M., & Maina, G. (2009). Human skin penetration of silver nanoparticles through intact and damaged skin. Toxicology, 255(1–2), 33–37.
- Lotfollahi, Z. (2024). The anatomy, physiology and function of all skin layers and the impact of ageing on the skin. *Wound Practice & Research, 32*(1), 6–10.
- Maquart, F. X., & Monboisse, J. C. (2014). Extracellular matrix and wound healing. Pathologie Biologie, 62(2), 91–95. doi:10.1016/j.patbio.2014.02.007

- Marambio-Jones, C., & Hoek, E. M. V. (2010). A review of the antibacterial effects of silver nanomaterials and potential implications for human health and the environment. Journal of Nanoparticle Research, 12(5), 1531–1551. https://doi.org/10.1007/s11051-010-9900-y
- McCormick, P. G., & Tsuzuki, T. (2002). Recent Developments in Mechanochemical Nanoparticle Synthesis. Materials Science Forum, 386-388, 377–386. doi:10.4028/www.scientific.net/msf.386-388.377
- Mohamed, H., & Hargest, R. (2022). Surgical anatomy of the skin. *Surgery (Oxford)*, *40*(1), 1–7. https://doi.org/10.1016/j.mpsur.2021.10.007
- Monteiro, D. R., Gorup, L. F., Silva, S., Negri, M., de Camargo, E. R., & Barbosa, D. B. (2022). Nanostructured silver vanquishes fungal biofilms: Development of silver-containing bioactive wound dressings. International Journal of Pharmaceutics, 597, 120306.
- Nagarjuna Reddy, V., Nyamathulla, S., Abdul Kadir, K., Mokhtar, S. I., Giribabu, N., & Pasupuleti, V. R. (2022). Gallocatechin-silver nanoparticles embedded in cotton gauze patches accelerated wound healing in diabetic rats by promoting proliferation and inhibiting apoptosis through the Wnt/β-catenin signaling pathway. PLOS ONE, 17(6), e0268505. https://doi.org/10.1371/journal.pone.0268505
- Neto, W. P., Oliveira, J. A., Soares, D. C. F., & Dantas, R. M. (2023). Synthesis of silver nanoparticles using green methods and their antimicrobial effects. Journal of Molecular Liquds, 384, 122067.
- Nourian Dehkordi, A., Babaheydari, F. M., Chehelgerdi, M., & Raeisi Dehkordi, S. (2019). Skin tissue engineering: Wound healing based on stem-cell-based therapeutic strategies. *Stem Cell Research & Therapy, 10*, 111. https://doi.org/10.1186/s13287-019-1227-7
- Oldenburg, S. J., Jackson, J. B., Westcott, S. L., & Halas, N. J. (2012). Infrared extinction properties of gold nanoshells. *Applied Physics Letters, 75*(19), 2897–2899.
- Pardhi, S., Bisen, P., Bawankar, S. A., Vishwakarma, A. K., Upadhyay, T., & Marwade, S. (2024). Fabrication of transdermal patches. International Journal for Multidisciplinary Research (IJFMR), 6(6), 1–5.
- Prausnitz, M. R., & Langer, R. (2008). Transdermal drug delivery. Nature Biotechnology, 26(11), 1261–1268. https://doi.org/10.1038/nbt.1504

- Proksch, E., Brandner, J. M., & Jensen, J. M. (2008). The skin: An indispensable barrier. Experimental Dermatology, 17(12), 1063–1072. https://doi.org/10.1111/j.1600-0625.2008.00786.x
- Rai, M., Yadav, A., & Gade, A. (2009). Silver nanoparticles as a new generation of antimicrobials. Biotechnology Advances, 27(1), 76–83. https://doi.org/10.1016/j.biotechadv.2008.09.002
- Rajeshkumar, S., & Malarkodi, C. (2014). Green synthesis and characterization of silver nanoparticles using Ocimum sanctum and their antibacterial activity. Pharmacognosy Research, 6(2), 123–129.
- Raziyeva, K., Kim, Y., Zharkinbekov, Z., Kassymbek, K., Jimi, S., & Saparov, A. (2021). Immunology of acute and chronic wound healing. *Biomolecules, 11*, 700. https://doi.org/10.3390/biom11050700
- Reinke, J. M., & Sorg, H. (2012). Wound repair and regeneration. *European Surgical Research, 49*, 35–43. https://doi.org/10.1159/000339613
- Rigo, C., Ferroni, L., Tocco, I., Roman, M., Munivrana, I., Gardin, C., ... & Zavan, B. (2013). Active silver nanoparticles for wound healing. International Journal of Molecular Sciences, 14(3), 4817–4840. https://doi.org/10.3390/ijms14034817
- Rybka, M., Mazurek, Ł., & Konop, M. (2023). Beneficial effect of wound dressings containing silver and silver nanoparticles in wound healing—From experimental studies to clinical practice. Life, 13(1), 69. https://doi.org/10.3390/life13010069
- Sedighi, O., Bednarke, B., Sherriff, H., & Doiron, A. L. (2024). Nanoparticle-based strategies for managing biofilm infections in wounds: A comprehensive review. *ACS Omega, 9*(26), 27853–27871. https://doi.org/10.1021/acsomega.4c01976
- Shankar, S. S., Rai, A., Ahmad, A., & Sastry, M. (2004). Rapid synthesis of Au, Ag, and bimetallic Au core–Ag shell nanoparticles using Neem (*Azadirachta indica*) leaf broth. *Journal of Colloid and Interface Science, 275*(2), 496–502. https://doi.org/10.1016/j.jcis.2004.03.003
- Sharma, V. K., Yngard, R. A., & Lin, Y. (2009). Silver nanoparticles: Green synthesis and their antimicrobial activities. Advances in Colloid and Interface Science, 145(1–2), 83–96
- Shimizu, H. (2017). Structure and function of the skin. In Shimizu's Dermatology (2nd ed., pp. 1–30). John Wiley & Sons. https://doi.org/10.1002/9781119146611.ch

- Singh, P., et al. (2022). Superior in vivo wound-healing activity of biosynthesized silver nanoparticles–nanogel on different wound models in rats. Applied Microbiology and Biotechnology.
- Singh, S., Bharti, A., & Meena, V. K. (2015). Green synthesis of multi-shaped silver nanoparticles: Optical, morphological and antibacterial properties. Journal of Materials Science: Materials in Electronics, 26(5), 3638–3648
- Song, J. Y., & Kim, B. S. (2009). Rapid biological synthesis of silver nanoparticles using plant leaf extracts. Bioprocess and Biosystems Engineering, 32(1), 79–84. https://doi.org/10.1007/s00449-008-0224-6
- Sportelli, M., Izzi, M., Volpe, A., Clemente, M., Picca, R., Ancona, A., ... & Cioffi, N. (2018). The pros and cons of the use of laser ablation synthesis for the production of silver nano-antimicrobials. *Antibiotics, 7*(3), 67. https://doi.org/10.3390/antibiotics7030067
- Sukweenadhi, J., Chandra, S. P., Setiawan, F., Avanti, C., Kartini, K., Koeswanto, A., & Yang, D. C. (2023). Wound healing effectiveness test of dermal patch formulated with green synthesized silver nanoparticles from Plantago major L. extract. Sarhad Journal of Agriculture, 39(S1), 11–22. https://doi.org/10.17582/journal.sja/2023/39/s1.11.22
- Suresh, A. K., Pelletier, D. A., Wang, W., Broich, M. L., Moon, J. W., Gu, B., ... & Doktycz, M. J. (2011). Silver nanocrystallites: Biofabrication using *Shewanella oneidensis*, and an evaluation of their comparative toxicity on Gram-negative and Gram-positive bacteria. *Environmental Science & Technology, 44*(13), 5210–5215. https://doi.org/10.1021/es903684r
- Taloni, A., Vodret, M., Costantini, G., & Zapperi, S. (2022). Size effects in micro and nanoscale materials fracture. *arXiv Preprint*, arXiv:2206.04469. https://doi.org/10.48550/arXiv.2206.04469
- Venus, M., Waterman, J., & McNab, I. (2010). Basic physiology of the skin. *Surgery (Oxford), 28*(10), 469–472. https://doi.org/10.1016/j.mpsur.2010.06.006
- Wallace, H. A. (2023). Wound healing phases. In *StatPearls*. StatPearls Publishing. https://www.ncbi.nlm.nih.gov/books/NBK535406/
- Wang, Z. L., Petroski, J. M., Green, T. C., & El-Sayed, M. A. (2005). Shape transformation and stability of monodisperse silver nanospheres. The Journal of Physical Chemistry B, 109(3), 421–426.

- Woo, Y. R., Cho, S. H., Lee, J. D., & Kim, H. S. (2022). The human microbiota and skin cancer. *International Journal of Molecular Sciences, 23*(3), 1813. https://doi.org/10.3390/ijms23031813
- Wysocki, A., Mustoe, T., & Schultz, G. (2006). Skin, molecular cell biology of. In *Encyclopedia of Molecular Cell Biology and Molecular Medicine* (Vol. 13, pp. 165–192). Wiley.
- Yeh, C.-J., Chen, C.-C., Leu, Y.-L., Lin, M.-W., Chiu, M.-M., & Wang, S.-H. (2017). The effects of artocarpin on wound healing: In vitro and in vivo studies. *Scientific Reports, 7*(1), 15599. https://doi.org/10.1038/s41598-017-15706-1
- Zielińska, A., Carreiró, F., Oliveira, A. M., Neves, A., Pires, B., Venkatesh, D. N., & Souto, E. B. (2020). Polymeric nanoparticles: Production, characterization, toxicology and ecotoxicology. *Molecules, 25*(16), 373. https://doi.org/10.3390/molecules25163773

Appendix 1

Preparation of Phosphate Buffer (KH_2PO_4, pH 5)

- **KH_2PO_4 Solution**: Accurately weigh 1.36 g of KH_2PO_4 and dissolve it in ~400 mL of distilled water in a 500 mL volumetric flask.
- **KOH Solution**: Prepare 0.1 M KOH by dissolving 5.611 g of KOH in 100 mL of distilled water.
- Add the KOH solution dropwise to the KH_2PO_4 solution under constant stirring. Monitor the pH using a calibrated pH meter until it reaches pH 5.0.
- Complete the volume to 500 mL with distilled water, mix thoroughly, and store at room temperature.

Appendix 2

Propofol 1% Dose and Injection Volume According to Body Weight in Wistar Rat

Rat Weight (g)	Injection Volume (mL)
268.0	2.01
270.0	2.02
308.0	2.31
271.0	2.03
261.0	1.96
267.0	2.0
273.0	2.05
260.0	1.95
269.0	2.02
278.0	2.08
238.0	1.78
257.0	1.93
278.0	2.08
258.0	1.94
253.0	1.9
253.0	1.9
267.0	2.0
279.0	2.09
258.0	1.94
250.0	1.88
261.0	1.96
268.0	2.01

الجمهورية الجزائرية الديمقراطية الشعبية
وزارة التعليم العالي والبحث العلمي

People's Democratic Republic of Algeria
Ministry of Higher Education and Scientific Research
Saad Dahleb University – Blida 1

Faculty of Natural and Life Sciences

Department of Biology

Final Year Thesis submitted in partial fulfillment of the requirements for the Master's Degree

Specialty: Pharmacotoxicology

Presented by:

NEMDIL Samira

Title:

Pharmacological Study of a Nanoencapsulated System and Histopathological Analysis

Defended before the jury:

Dr. RAHIM I.	University of Blida 1	**Chairperson**
Dr. BOULESNAM L. S.	University of Blida 1	**Examiner**
Dr. AYACHI N.	University of Blida 1	**Supervisor**
PhD Candidate BOULAIOUNE A.	University of Blida 1	**Co-supervisor**

Academic year: **2024-2025**

Boulesnam saliha Lydia

الجمهورية الجزائرية الديمقراطية الشعبية
وزارة التعليم العالي والبحث العلمي

People's Democratic Republic of Algeria
Ministry of Higher Education and Scientific Research
Saad Dahleb University – Blida 1

Faculty of Natural and Life Sciences

Department of Biology

Final Year Thesis submitted in partial fulfillment of the requirements for the Master's Degree

Specialty: Pharmacotoxicology

Presented by:

NEMDIL Samira

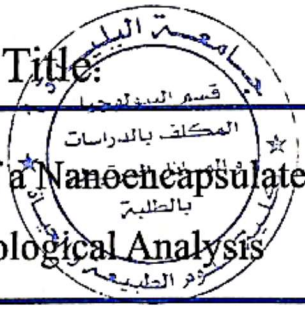

Title:

Pharmacological Study of a Nanoencapsulated System and Histopathological Analysis

Defended before the jury:

Dr. RAHIM I.	University of Blida 1	**Chairperson**
Dr. BOULESNAM L. S.	University of Blida 1	**Examiner**
Dr. AYACHI N.	University of Blida 1	**Supervisor**
PhD Candidate BOULAIOUNE A.	University of Blida 1	**Co-supervisor**

Academic year: **2024-2025**

Boulesnam saliha Lydia